Biointerface Research in Applied Chemistry
Platinum Open Access Journal (ISSN: 2069-5837)

Article
Volume 11, Issue 5, 2021, 13064 - 13088
https://doi.org/10.33263/BRIAC115.1306413088

Theoretical DFT Studies on Free Base, Cationic and Hydrochloride Species of Narcotic Tramadol Agent in Gas Phase and Aqueous Solution

José Ruiz Hidalgo [1], Silvia Antonia Brandán [1,*]

[1] Cátedra de Química General, Instituto de Química Inorgánica, Facultad de Bioquímica, Química y Farmacia, Universidad Nacional de Tucumán, Ayacucho 471, 4000, San Miguel de Tucumán, Tucumán, Argentina
* Correspondence: silvia.brandan@fbqf.unt.edu.ar; sbrandan@fbqf.unt.edu.ar;

Scopus Author ID 6602262428

Received: 4.01.2021; Revised: 27.01.2021; Accepted: 29.01.2021; Published: 7.02.2021

Abstract: Theoretical studies based on the density functional theory (DFT) have been performed to study structural and vibrational properties of the free base, cationic, and hydrochloride species of narcotic tramadol agent in the gas phase and aqueous solution. In both media, B3LYP/6-31G* calculations were used while in solution, the self-consistent reaction field (SCRF) method together with the integral equation formalism variant polarised continuum (IEFPCM) and universal solvation model density (SMD) models have been employed because these models consider the solvent effects. The vibrational studies have revealed that the species cationic is present in the solid phase because the most intense band predicted for the hydrochloride in infrared and Raman spectra is not observed in the experimental spectra. The harmonic force fields, together with the normal internal coordinates and scaling factors, have allowed the complete vibrational assignments of 126, 129, and 132 vibration modes expected for the free base, cationic, and hydrochloride species, respectively, by using the SQMFF methodology. The cationic species evidence the most negative solvation energy and higher hydration in solution in agreement with its lower stability, while the hydrochloride species is the most reactive in solution. MK charges and NBO and AIM studies support cationic species' instability due to the positive charge on N atom. Comparisons of the experimental UV spectrum of hydrochloride tramadol with the predicted for the three species suggest that the free base, cationic, and hydrochloride species can be present in solution. Comparisons of predicted infrared, Raman, ^{1}H, and ^{13}C NMR and electronic spectra for the free base, cationic, and hydrochloride species of tramadol with the corresponding experimental ones have evidenced reasonable correlations for the cationic species showing that this species present in the solid phase and in solution.

Keywords: tramadol; molecular structure; DFT calculations; vibrational spectra.

© 2021 by the authors. This article is an open-access article distributed under the terms and conditions of the Creative Commons Attribution (CC BY) license (https://creativecommons.org/licenses/by/4.0/).

1. Introduction

In pharmacology, the hydrochloride species are highly used as medicaments because these structural forms allow the oral bioavailability of drugs as bioactive molecules and their incorporation quickly as therapeutic agents, as mentioned by Veber *et al*. [1]. Other important factors must be taken into account in the design of new drugs, such as the presence of hydrogen bond acceptors and donor groups, as reported by Lipinski *et al*. [2]. Theoretical studies combined with experimental results have evidenced that in some antiviral, alkaloids, and narcotic species as well as in antihistaminic and anti-hypertensive agents, the free base and cationic forms should be studied together with the hydrochloride one because, in aqueous

solution, the hydrochloride species is in its cationic form while the free base as cationic one [3-23]. In this work, the free base, cationic, and hydrochloride forms of narcotic tramadol were studied from a theoretical point of view combining DFT calculations with experimental available infrared, Raman, ^{1}H- and ^{13}C-NMR and ultraviolet spectra in order to predict structural, electronic, topological and vibrational properties of its three forms [24]. In the free base, the N atom is a tertiary amine with three organic substituents, while the cationic has four organic substituents and, for this reason, it is a quaternary ammonium cation with a charged nitrogen center, as can be seen in Figure 1. The Cl anion neutralizes the quaternary charged cation in the hydrochloride form, and its species is uncharged.

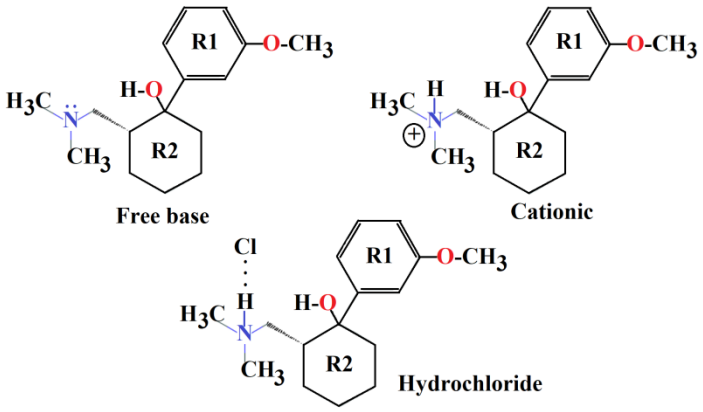

Figure 1. Structures of the free base, cationic, and hydrochloride forms of tramadol.

Then, complete vibrational assignments of those three forms of tramadol were performed by using the B3LYP/6-31G* method [25,26] with the scaled quantum mechanical force fields (SQMFF) methodology, normal internal coordinates, transferable scaling factors, and the Molvib program [27-29]. A systematic chemical name of tramadol is (1RS,2RS)-2-[(Dimethylamino)methyl]-1-(3-methoxyphenyl) cyclohexanol hydrochloride [30], while the experimental structure of tramadol hydrochloride was determined by X-ray diffraction by Kaduk *et al*. [31]. Other structures of Tramadol hydrochloride-benzoic acid (1/1) and of Tramadol hydrochloride and its acetonitrile solvate were also reported by Siddaraju *et al*. [32] and by Bag and Reddy [33], respectively. The physics and chemical properties of tramadol hydrochloride are known as well as its stability, pharmacokinetics, and metabolism, and, so far, only some vibration modes were published for this form of tramadol [24]. After optimizing three species in the gas phase and aqueous solution, the structural, electronic, topological, and vibrational properties were obtained together with their reactivities and behaviors in the two studied media. Later, the complete assignments of expected 126, 128, and 132 vibration modes of the free base, cationic, and hydrochloride forms of tramadol are reported together with the harmonic force fields the scaled force constants. The three forms of tramadol have the N-$(CH_3)_2$·group in its structures, as in antihistaminic promethazine and diphenydramine agents [10,15], while in some alkaloids an only N-CH_3 group is found [8-11,16]. Hence, these N-CH3 groups' presence plays a very important role in the chemical properties and biological activities of these pharmacological species. Here, comparisons of predicted infrared, Raman, ^{1}H-, ^{13}C-NMR, and ultraviolet-visible spectra of hydrochloride species of tramadol with the corresponding experimental ones show good correlations [24].

2. Materials and Methods

Firstly, the initial structure of the free base of tramadol was modeled with the *GaussView* program [34]. Then, to its structure was added an H atom to form the cationic later, to optimized cation was added a Cl atom to form the hydrochloride species. The three species were optimized in the gas and aqueous solutions with the Gaussian 09 program [35] and the B3LYP/6-31G* level of theory [25,26]. The self-consistent reaction force (SCRF) method was used to perform calculations in solution because this method, together with the integral equation formalism variant polarised continuum (IEFPCM) and universal solvation model density (SMD) models, consider the solvent effects [36-38]. The three structures of tramadol have two six member's rings, as shown in scheme 1. One of these rings is a methoxyphenyl, which is identified as R1, and the other one cyclohexanol, designed as R2. These identifications are important to perform the vibrational study by using the normal internal coordinates. The scaled quantum mechanical force fields (SQMFF) methodology and the Molvib program have allowed the determinations of harmonic force fields by using transferable scaling factors [27-29]. After that, three species of tramadol's complete vibrational assignments were performed considering normal vibration modes potential energy distribution (PED) contributions ≥ 10 %. Good correlations were observed between the infrared and Raman spectra, particularly in the latter spectrum, when recognized equations were used to correct intensities activities [39,40]. Here, atomic charges, bond orders, molecular electrostatic potentials, stabilization energies, and topological properties were evaluated for the three species of tramadol in the two media by using natural bond orbital (NBO), atoms in molecules (AIM) calculations, and the Merz-Kollman (MK) scheme [41-44]. The *GaussView* and Moldraw programs were used to obtain the mapped MEP surfaces and volume variations of those three tramadol species [34,45]. In order to evaluate reactivities and behaviors of three species of tramadol, the frontier orbitals were employed to calculate the energy gap values and the chemical potential (μ), electronegativity (χ), global hardness (η), global softness (S), global electrophilicity index (ω) and global nucleophilicity index (E) descriptors [3-17,46]. The ^{1}H and ^{13}C NMR and electronic spectra were predicted in aqueous solution by using the gauge-including atomic orbital (GIAO) method and the Time-dependent DFT calculations (TD-DFT) by using the same level of theory [35,47].

3. Results and Discussion

3.1. Geometrical parameters and properties in both media.

In Figure 2 are presented the optimized molecular structures of free base, cationic, and hydrochloride species of tramadol and atoms labeling while the R1 and R2 rings are shown in yellow and green colors. Some predicted properties for the tree species of tramadol in the gas phase and aqueous solution with the B3LYP/6-31G* method can be seen in Table 1. Thus, energy values, dipole moments, volumes, and variations are shown for each different media species. Note that in Table 1 the total E corrected by zero points vibrational energy (ZPVE) is also presented. The results show that the three species in solution increase the dipole moments values while only in the cationic species is observed a contraction of volume in this medium because the other two species evidence expansions in solution. The higher volume variation is observed in the hydrochloride species in solution. It shows a higher expansion of volume and

dipole moment value due to its higher hydration with water molecules. The size of Cl atom influences on those two properties.

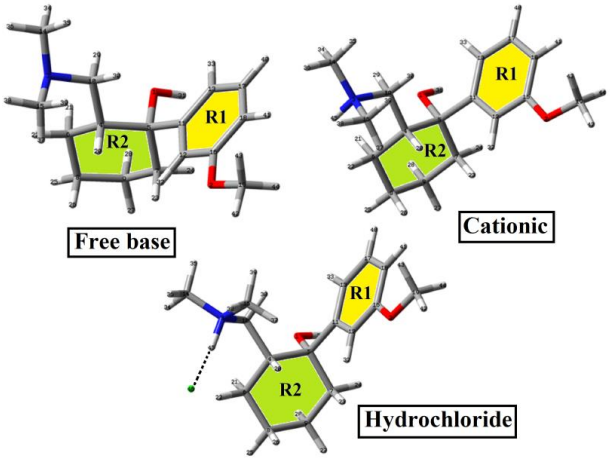

Figure 2. Molecular structures of the free base, cationic, and hydrochloride species of tramadol and atoms labeling. The two rings are shown in different colors.

Table 1. Calculated total energies (*E*), dipole moments (μ) and volumes (V) of the free base, cationic, and hydrochloride species of tramadol in the gas phase and aqueous solution by using the B3LYP/6-31G* method.

B3LYP/6-31G* Method					
Medium	E (Hartrees)	E_{ZPVE} (Hartrees)	μ (D)	V (Å^3)	ΔV (Å^3)
Free Base					
GAS	-829.9342	-829.5432	2.48	306.1	0.3
PCM/Water	-829.9462	-829.5547	3.85	306.4	
Cationic					
GAS	-833.3306	-829.9239	10.06	310.9	1.0
PCM/Water	-830.4196	-830.0125	12.32	309.9	
Hydrochloride					
GAS	-1290.7572	-1290.3523	10.06	333.2	7.5
PCM/Water	-1290.7939	-1290.3871	16.38	340.7	

Suppose now the positions and orientations of dipole moment values for the three species of tramadol in the gas phase are analyzed from Figure 3. In that case, important differences are observed in the tree species. For instance, in the free base, the vector is oriented from the C4 atom belonging to R2 ring to C16 atom linked to O-CH_3 group, between the OH and O-CH_3 groups, while in the cationic form, its vector is oriented from the C11 atom belonging to R1 toward the positively charged N3 atom. As in the free base, the dipole moment vector of hydrochloride species is directed from the C4 atom belonging to R2 ring to C17 atom belonging to R1 ring, between the OH and O-CH_3 groups, in opposition to Cl atom. In solution, only changes in the magnitudes of dipole moments for the tree species are observed. The different values of dipole moment values in solution indicate that the three species are hydrated in different ways in aqueous solution, as evidenced in the volume variations. Hence, these changes are attributed to the different solvation energies, as was observed in various structural studies on the free base, cationic and hydrochloride species of some alkaloids, antihistaminic, anti-hypertensive and antiviral agents the cationic species [3-5,7,9-19,22,23]. Hence, the determinations of corresponding solvation energies are important in these three species of tramadol.

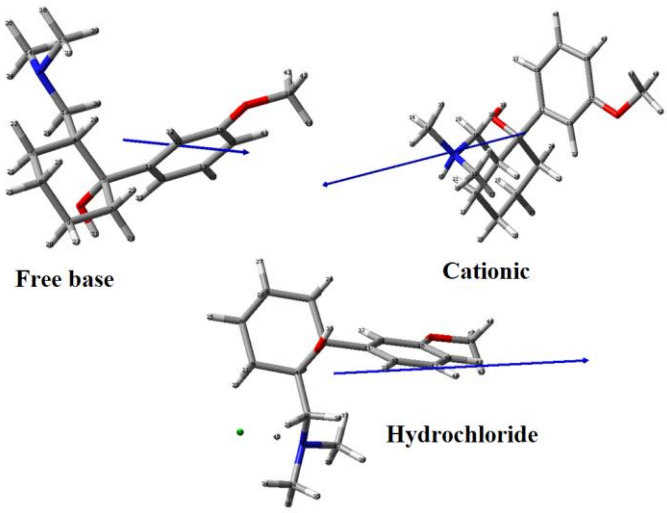

Figure 3. Orientations and directions of dipole moment vectors for the free base, cationic and hydrochloride species of tramadol in the gas phase by using the B3LYP/6-31G* method.

Table 2 summarizes corrected solvation energies by the total non-electrostatic terms and by zero points vibrational energy (ZPVE) for the free base, cationic, and hydrochloride species tramadol in the gas phase and aqueous solution by using the B3LYP/6-31G* method. Here, the results show a high ΔG_c value for the cationic form of tramadol, in agreement with some alkaloids, antihistaminic, anti-hypertensive, and antiviral agents [3-5,7,9-19,22,23]. The positively charged cationic species evidence higher hydration in the solution.

Table 2. Corrected solvation energies by the total non-electrostatic terms and by zero-point vibrational energy (ZPVE) of the free base, cationic, and hydrochloride species of Tramadol in the gas phase and aqueous solution by using the B3LYP/6-31G* method.

B3LYP/6-31G* method[a]			
Solvation energy (kJ/mol)			
Medium	$\Delta G_{un}^{\#}$	ΔG_{ne}	ΔG_c
Free Base			
PCM/Water	-30.16	22.02	-52.18
Cationic			
PCM/Water	-232.39	34.90	-267.29
Hydrochloride			
PCM/Water	-91.28	32.18	-123.46

$\Delta G_{un}^{\#}$= uncorrected solvation energy, ΔG_{ne}= total non electrostatic terms, ΔG_c= corrected solvation energies. [a]This work

When the ΔG_c values for the three species of tramadol are compared in Table 3 with the values for other species with different biological activities such as alkaloids, antihistaminic and antiviral agents by using the B3LYP/6-31G* method, we observed that in all cases, the cationic species evidence higher ΔG_c values due to that the positive charges on N atoms produce higher hydrations in aqueous solution. The behaviors of ΔG_c of these species can be seen in Figure 4. Note that the species of tramadol are indicated as (Tra), amadantine or amantadine as (A) [23], naloxone (N) [16], R(+) forms of promethazine (P) [15], cyclizine (Cy) [11], morphine (M) [3], cocaine (Co) [5], scopolamine (S) [9], heroin (H) [7] and tropane (Tro) [4,23]. Figure 4 shows that the ΔG_c values for all free base and hydrochloride species follow approximately the same tendencies while the hydrochloride ones show different behavior.

Table 3. Corrected solvation energies by the total non-electrostatic terms and zero-point vibrational energy (ZPVE) of different species in aqueous solution using the B3LYP/6-31G* method.

B3LYP/6-31G* method				
Solvation energy (kJ/mol) ΔG_c				
Nº	Species	Free base	Cationic	Hydrochloride
1	Tramadol[a]	52.18	-267.29	-123.46
2	Amantadine[b]	-23.07	-276.35	-115.03
3	Naloxone[c]	-100.75	-302.45	-122.28
4	R(+)-Promethazine[d]	-17.87	-262.81	-52.02
5	Cyclizine[e]	-29.53	-244.36[#]	-105.06
6	Morphine[f]	-60.91	-309.19	-144.74
7	Cocaine[g]	-71.26	-255.24	-138.14
8	Scopolamine[h]	-75.47	-310.34	-122.74
9	Heroin[i]	-88.67	-323.14	-161.94
10	Tropane[b,j]	-12.55	-244.33	-87.18

ΔG_c= corrected solvation energies, [a]This work, [b]From Ref [23], [c]From Ref [16], [d]From Ref [15], [e]From Ref [11], [f]From Ref [3], [g]From Ref [5], [h]From Ref [9], [i]From Ref [7], [j]From Ref [4,23], [#]Cation cyclizine: 6-31+G*

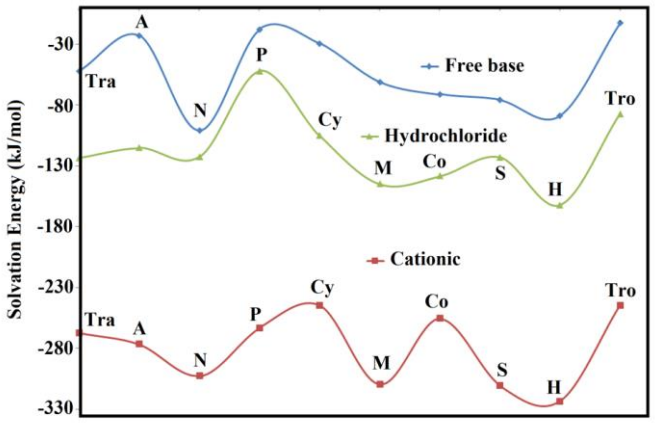

Figure 4. Comparisons of corrected solvation energies of the free base, cationic, and hydrochloride species of tramadol corresponding to alkaloids, antihistaminic and antiviral agents by using the B3LYP/6-31G* method.

On the contrary, the cationic species are most hydrated in aqueous solution and, hence, the ΔG_c values are highly negative, evidencing the highest negative value of the species of heroin. Thus, the free base of naloxone and the cationic and hydrochloride species of heroin have the most negative values, while the free base and cationic species of tropane and the hydrochloride one of promethazine present the lowest values. On the other side, the cationic form of naloxone shows approximately a similar value to morphine and scopolamine species. Studies in a solution of antiviral agents have suggested that the presence of acceptors and donors groups in the structures play an important role in the ΔG_c values [23]. Hence, the lower ΔG_c values observed for the free base and cationic species of tropane, amantadine, or cyclicine probably could be attributed to the presence of only a tertiary and/or quaternary N atoms belong to >N-CH_3 groups while in the compared species, other acceptors and donors groups are present in its structures in addition to N atoms [4,8,11,23].

Comparisons of geometrical parameters for the three tramadol species using the B3LYP/6-31G* method with the corresponding experimental values determined for the crystal structure of tramadol hydrochloride by Kaduk *et al*. can be seen in Table 4 [31].

Note that the root-mean-square deviation (RMSD) values are used to compare bond lengths and angles. In general, good correlations between theoretical and experimental results were found for the three tramadol species with RMSD values of 0.017-0.010 Å for bond lengths and of 1.61-1.54 º for bond angles.

Table 4. Comparisons between calculated geometrical parameters for the three Tramadol species in the gas phase and aqueous solution with the corresponding experimental ones.

Parameters	B3LYP/6-31G* Method[a]						Experimental[b]
	Free Base		Cationic		Hydrochloride		
	Gas	PCM	Gas	PCM	Gas	PCM	
Bond lengths (Å)							
O1-C5	1.437	1.441	1.433	1.438	1.436	1.438	1.430
C5-C11	1.538	1.539	1.537	1.539	1.539	1.539	1.546
C5-C7	1.551	1.549	1.546	1.548	1.549	1.548	1.542
C5-C4	1.558	1.561	1.566	1.562	1.558	1.562	1.563
C7-C9	1.533	1.532	1.533	1.532	1.533	1.532	1.510
C9-C8	1.533	1.531	1.532	1.531	1.532	1.531	1.529
C8-C6	1.533	1.533	1.536	1.534	1.532	1.533	1.529
C6-C4	1.540	1.541	1.543	1.543	1.543	1.541	1.542
C4-C10	1.541	1.540	1.534	1.534	1.543	1.534	1.547
C10-N3	1.467	1.473	1.525	1.515	1.504	1.511	1.514
N3-C14	1.456	1.463	1.503	1.499	1.485	1.495	1.475
N3-C15	1.456	1.463	1.502	1.498	1.487	1.493	1.487
C11-C12	1.397	1.399	1.397	1.398	1.398	1.398	1.392
C11-C13	1.403	1.403	1.403	1.403	1.404	1.403	1.392
C13- C17	1.392	1.394	1.394	1.394	1.393	1.394	1.392
C17-C18	1.396	1.396	1.394	1.396	1.395	1.396	1.417
C18-C16	1.399	1.399	1.401	1.399	1.400	1.399	1.392
C16-C12	1.400	1.400	1.402	1.401	1.401	1.401	1.392
C16-O2	1.367	1.375	1.358	1.374	1.364	1.374	1.367
O2-C19	1.417	1.429	1.425	1.429	1.419	1.429	1.440
RMSD[b]	**0.017**	**0.014**	**0.013**	**0.011**	**0.010**	**0.010**	
Bond angles (°)							
O1-C5-C11	110.62	110.50	111.39	110.74	110.58	110.68	109.7
O1-C5-C7	108.80	108.76	109.65	109.19	109.43	109.19	110.8
O1-C5-C4	105.46	105.95	103.91	105.56	104.71	105.67	104.4
C5-C7-C9	113.03	113.03	113.01	113.04	113.15	113.07	111.9
C7-C9-C8	110.71	110.64	110.82	110.76	110.67	110.71	112.5
C7-C5-C11	109.73	109.31	110.82	109.71	110.07	109.62	109.0
C7-C5-C4	110.25	110.48	110.04	110.04	110.45	110.14	109.8
C9-C8-C6	110.85	111.26	110.99	111.21	111.00	111.12	108.5
C8-C6-C4	112.72	112.86	112.21	112.27	112.30	112.47	113.0
C6-C4-C5	111.39	111.42	111.68	111.52	112.00	111.56	110.1
C6-C4-C10	110.86	112.18	112.29	112.35	110.63	112.23	111.9
C5-C4-C10	111.85	110.93	107.91	109.40	110.92	109.64	109.5
C4-C10-N3	112.99	115.32	113.83	114.42	112.78	115.54	114.2
C10-N3-C14	111.58	108.67	111.18	110.52	112.44	109.58	111.7
C10-N3-C15	112.51	111.32	112.91	113.36	112.59	113.70	112.2
C14-N3-C15	110.51	109.24	111.21	110.72	111.01	110.42	113.2
C4-C5-C11	111.84	111.74	110.80	111.47	111.44	111.43	113.0
C5-C11-C12	120.58	120.20	120.21	120.18	120.55	120.18	120.1
C5-C11-C13	120.94	121.32	120.90	121.17	120.94	121.25	120.0
C11-C13-C17	120.26	120.26	119.90	120.15	120.23	120.18	121.2
C13-C17-C18	121.30	121.37	121.35	121.37	121.30	121.38	118.2
C17-C18-C16	118.69	118.51	119.00	118.59	118.75	118.54	120.6
C18-C16-C12	120.06	120.29	119.74	120.25	120.00	120.27	120.0
C16-C12-C11	121.20	121.07	121.11	120.99	121.18	121.03	120.0
C12-C11-C13	118.46	118.46	118.88	118.62	118.50	118.56	120.0
C16-O2-C19	118.20	117.87	118.63	117.88	118.40	117.96	116.4
O2-C16-C18	124.60	124.27	124.92	124.30	124.67	124.35	122.7
O2-C16-C12	115.32	115.42	115.33	115.43	115.31	115.37	112.2
RMSD[b]	**1.59**	**1.77**	**1.59**	**1.54**	**1.57**	**1.62**	
Dihedral angles (°)							
C19-O2-C16-C18	-0.06	-1.99	-3.74	-2.47	-0.78	3.27	
C19-O2-C16-C12	179.75	177.90	176.32	177.43	179.19	-176.80	
C14-N3-C10-C4	-158.43	-173.91	-166.88	-171.66	-151.75	-179.03	
N3-C10-C4-C5	-174.16	-178.27	179.31	-175.84	-146.12	-169.17	
O1-C5-C7-C9	-61.29	-61.91	-59.73	-61.28	-61.79	-61.66	
O1-C5-C11-C12	-176.16	-179.32	-178.70	-179.85	-177.09	179.38	

[a]This work, [b]Ref [31]

The better correlations in bond lengths are observed for the hydrochloride species, as expected because the experimental data were determined for this species. The two N3-C14 and N3-C15 distances correspond to the >N-$(CH_3)_2$ groups are predicted with similar values in the three species and both media. Studies related to the behavior of bonds N-CH_3 lengths in some alkaloids, narcotics, and anti-histaminic agents in the gas phase and aqueous solution have evidenced that there are some correlations in their properties [8]. Hence, in Table 5 it is observed bond lengths between the N and C atoms of the N-CH_3 bonds belonging to the three tramadol species in the gas phase and aqueous solution by using B3LYP/6-31G* calculations. The results are compared in the same table with published for amadantine [23], naloxone [16], promethazine [15], cyclizine [11], cocaine [3], morphine [5], scopolamine [9], heroin [7] and tropane [4,23] at the same level of theory. The hydrochloride forms of all the species were studied, except for scopolamine that was studied in its hydrobromide form [9].

Table 5. Bonds lengths observed between the N and C atoms of the N-CH_3 bonds belonging to the three tramadol species in the gas phase and in aqueous solution by using B3LYP/6-31G* calculations.

Species	N-CH_3 bond					
	Gas-phase			Aqueous solution		
	Free base	Cationic	Hydrochloride	Free base	Cationic	Hydrochloride
Tramadol[a]	1.456	1.503	1.486	1.463	1.498	1.494
Amantadine[b]	1.469	1.550	1.501	1.476	1.516	1.510
Naloxone[c]	1.459	1.468	1.523	1.517	1.513	1.521
R(+)-promethazine[d]	1.460	1.508	1.487	1.468	1.501	1.496
Cyclizine[e]	1.453	1.453	[#]	1.459	[#]	1.489
Morphine[f]	1.453	1.500	1.483	1.460	1.497	1.493
Cocaine[g]	1.459	1.493	1.487	1.467	1.492	1.494
Scopolamine[h,γ]	1.462	1.492	1.491	1.466	1.491	1.493
Heroin[i]	1.453	1.501	1.483	1.460	1.498	1.492
Tropane[j]	1.458	1.496	1.478	1.467	1.491	1.486

[a]This work, [b]From Ref [23], [c]From Ref [16], [d]From Ref [15], [e]From Ref [11], [f]From Ref [3], [g]From Ref [5], [h]From Ref [9], [i]From Ref [7], [j]From Ref [4,23], [#]Imaginary frequencies, [γ]Hydrobromide.

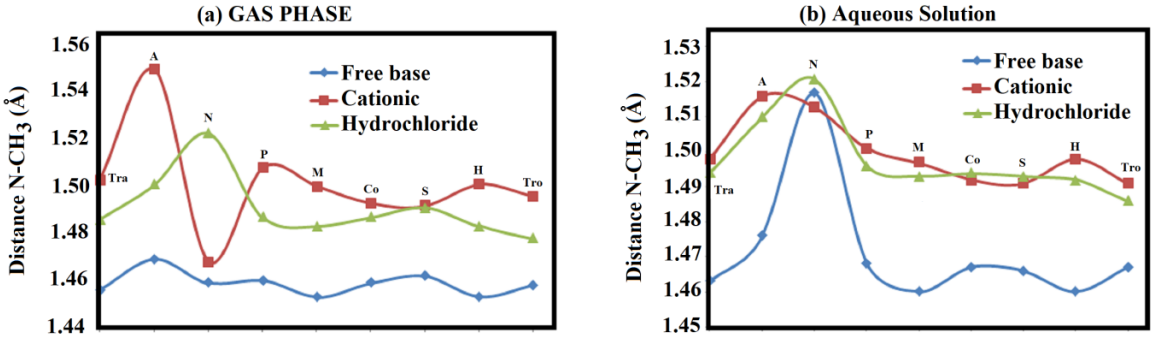

Figure 5. Bonds lengths observed between the N and C atoms of the N-CH_3 bonds belonging to the three tramadol species in the gas phase (a) and aqueous solution (b) by using B3LYP/6-31G* calculations compared with amadantine [23], naloxone [16], promethazine [15], cyclizine [11], cocaine [3], morphine [5], scopolamine [9], heroin [7] and tropane [4,23].

Figure 5 graphed the distances between N and C atoms of N-CH_3 groups for all compared species where their names have the same notation presented in Figure 4. The cyclizine species were not presented here because the cationic form in the gas phase and the hydrochloride one in solution present imaginary frequencies at the B3LYP/6-31G* level [11].

Here, it is necessary to clarify that the distance values presented in Table 5 for promethazine and tramadol correspond to average values because these species have two N-$(CH_3)_2$ groups. When Fig.5a is analyzed, we observed the lower distances for all free base species in the gas phase, showing values between 1.47 and 1.45 Å while the presence of

positive charges on the N atoms in all cationic species increases the distances slightly to values between 1.47 and 1.55 Å. The cationic species of amantadine and naloxone evidence the highest and lowest values, respectively, while the remaining species present values between 1.49 and 1.51 Å. These differences are quickly justified because in amantadine, the group is N-CC_3 group, while in naxolone is an allyl >N-CH_2-CH=CH_2 group different from the N-CH_3 group. On the other side, the hydrochloride species of naloxone present a higher value in the gas phase, while the tropane species present a lower value. In solution, the situation change because the cationic and hydrochloride species of all compared compounds reveal approximately the same behaviors and, where the cationic species of amantadine and the hydrochloride one of naloxone have the higher values. The similar behaviors for the cationic and hydrochloride species could indicate that the hydrochloride forms are as cationic ones in aqueous solution, while the differences observed between amantadine and naloxone could be justified by the presence of groups linked to quaternary N atoms different from N-CH_3, which are present in the other species. The free base of naloxone has a higher distance in solution due to the size of the allyl >N-CH_2-CH=CH_2 group. For the other species, the distances are around 1.47 and 1.46 Å. These different values in the N-C distance evidence clearly that the groups linked to tertiary (free base species) or quaternary N atoms (cationic and hydrochloride species) affect the distances and, hence, on some properties of the compound.

3.2. Atomic charges, molecular electrostatic potentials, and bond orders in both media.

Previous structural and vibrational studies of pharmacological hydrochloride species with different biological activities have revealed that the hydrochloride species in aqueous solution are present in this medium as cationic ones [3-5,7,9-12,15-20,22,23] and, for these reasons, atomic charges, molecular electrostatic potentials (MEP), and bond orders (BO) are important properties that explain the behaviors of these species in different media.

Table 6. Mulliken, Merz-Kollman, and NPA charges (a.u.), molecular electrostatic potentials (MEP) (a.u.) and bond orders (BO), expressed as Wiberg indexes of three tramadol species in the gas phase and aqueous solution by using B3LYP/6-31G* calculations.

Free base										
	Gas Phase					**PCM**				
Atoms	MK	Mulliken	NPA	MEP	BO	MK	Mulliken	NPA	MEP	BO
1 O	-0.639	-0.655	-0.763	-22.318	1.795	-0.615	-0.655	-0.763	-22.318	1.793
2 O	-0.335	-0.509	-0.523	-22.285	2.121	-0.339	-0.516	-0.525	-22.286	2.114
3 N	-0.168	-0.370	-0.504	-18.368	3.116	-0.228	-0.376	-0.496	-18.368	3.110
Cationic										
Atoms	MK	Mulliken	NPA	MEP	BO	MK	Mulliken	NPA	MEP	BO
1 O	-0.620	-0.662	-0.387	-22.199	1.785	-0.597	-0.661	-0.772	-22.201	1.784
2 O	-0.335	-0.506	-0.259	-22.195	2.135	-0.337	-0.513	-0.521	-22.197	2.124
3 N	0.292	-0.492	-0.221	-18.061	3.470	0.251	-0.489	-0.440	-18.058	3.471
Hydrochloride										
Atoms	MK	Mulliken	NPA	MEP	BO	MK	Mulliken	NPA	MEP	BO
1 O	-0.634	-0.656	-0.766	-22.301	1.792	-0.624	-0.654	-0.764	-22.295	1.793
2 O	-0.311	-0.505	-0.519	-22.272	2.128	-0.327	-0.514	-0.524	-22.267	2.118
3 N	0.539	-0.476	-0.487	-18.254	3.361	0.539	-0.476	-0.470	-18.229	3.397

For the three studies, the results only for the O1, O2, and N3 atoms corresponding to groups donor (OH) and acceptors (O-CH_3 and N-$(CH_3)_2$) H bonds, respectively, are presented in Table 6. Hence, atomic Merz-Kollman (MK), Mulliken, and natural population (NPA) charge for the three tramadol species in both media by using the B3LYP/6-31G* method are given in Table 6, while Figure 6 are shown the behaviors of three charges on those three atoms of free base, cationic and hydrochloride species of tramadol in both media. An exhaustive

inspection of graphic show different behaviors of three types of charges but the same in both media.

Thus, from the three different studied charges, only the MK ones evidence positive charges on N3 atoms of cationic and hydrochloride species in both media, as expected because these two species have four organic substituents and quaternary ammonium cations while the Mulliken and NPA charges on these atoms show negative values.

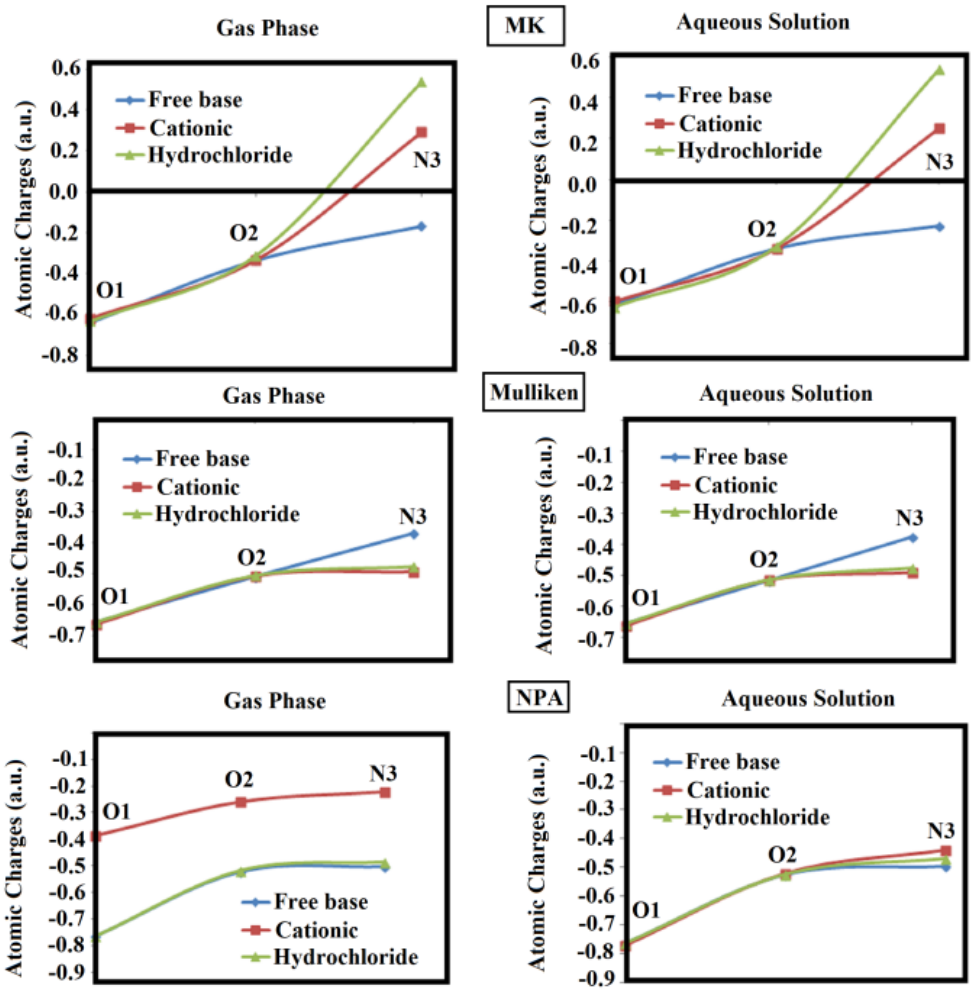

Figure 6. Behaviors of MK, Mulliken, and NPA charges on O1, O2 and N3 atoms of the free base, cationic, and hydrochloride species of tramadol in both media by using B3LYP/6-31G* calculations.

Negative MK charges are observed on N3 atoms of the free base in both media due to its pairs electrons available, while only the Mulliken charges on N3 of cationic and hydrochloride species have the same negative values. On the other hand, the behaviors of NPA charges for the three species of tramadol in the gas phase are different form in aqueous solution; thus, the three atoms of cationic species show values very high in the gas phase, as compared with the other two ones. In solution, the same NPA charges on the O1 and O2 atoms of three species are observed, while on N3 of cationic species, a slightly higher NPA charge is evidenced. Finally, the three types of charges reveal negative values on O1 and O2 atoms of three species in both media.

Regarding the molecular electrostatic potentials (MEP) on three O1, O2, and N3 atoms of three tramadol species from Table 6 carefully, we observed practically the same values for the free base in both media and, only slight changes are observed for the other two species,

evidencing few variations on O2 and N3 of hydrochloride species in solution (0.025-0.005 a.u.). However, when the mapped MEP surfaces are built for the three species in the gas phase with the *GaussView* program [34], different regions and colorations are observed, as shown in Figure 7. The free base shows strong blue colors on H31, which belongs to O1-H31 group, while red colorations are observed on O1, O2, and N3 atoms that belong to OH, O-CH_3, and N-$(CH_3)_2$ groups, respectively. The cationic species show strong blue color on the N-$(CH_3)_2$ groups due to the charge on N3, as expected because its species is positively charged, while the light blue color on the remaining atoms of a molecule. The hydrochloride species shows an extensive and strong red region around Cl atom and the other two orange regions on O1 and O2, while the strong blue color is observed on the H31 atom that belongs to OH group.

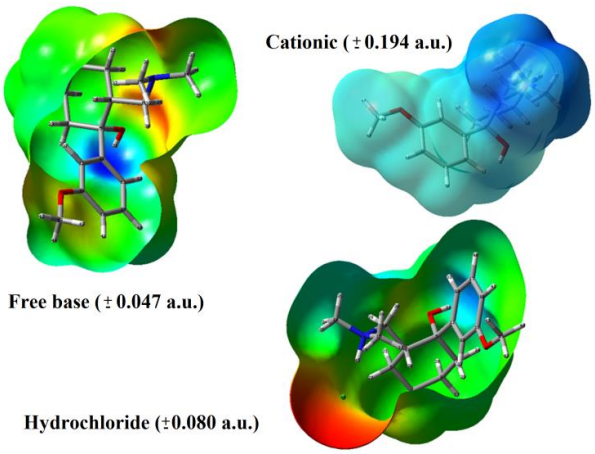

Figure 7. Calculated electrostatic potential surfaces on the molecular surfaces of the free base, cationic, and hydrochloride species of tramadol in the gas phase. B3LYP functional and 6-31G* basis set. Isodensity value of 0.005.

Hence, the nucleophilic and/or electrophilic sites are evidenced in the three species by the red and blue colors, respectively, and, also, by the different calculated MEPs values. These mapped MEP surfaces are completely different in the three tramadol species and reveal regions in which reactions with potential biological electrophiles or nucleophiles occur.

Other interesting properties predicted for the three tramadol species with the NBO program by using the B3LYP/6-31* level of theory are the bond orders (BOs) totals by atom, expressed as Wiberg indexes [25,26]. Table 6 shows that O2 and N3 of cationic species present higher BOs values than O1 of the other two species. Note that O1 in the three species have the lower values, as expected, because this atom belongs to OH group and, for these reasons, these are the most labile. In the cationic species, the N3 has a higher BO value due to its charge. In solution, the BOs for the three species evidencing a decrease due to donors and acceptors groups' hydrations. Nevertheless, when the Wiberg bond index matrix in the Natural Atomic Orbital (NAO) basis for the H45-Cl46 bond is investigated for the hydrochloride species of tramadol it is observed a value of 0.343 in gas phase indicating a covalent character for this bond but, in solution, the value change to 0.213 because the character of bond slightly changes to ionic (N3-H45⋯ Cl46). A similar resulted was observed in the hydrochloride species of antiviral amantadine [23].

3.3. NBO and AIM studies.

The hydration in an aqueous solution of OH, O-CH_3, and N$(CH_3)_2$ groups in the three species of tramadol could generate different types of interactions, which can be important,

taking into account its stabilities and its use as a pharmacological drug [1,2]. Hence, the presence of a different type of interactions in those species has been studied with the NBO program using the second-order perturbation theory analyses of the Fock matrix in NBO Basis and with the AIM 2000 program by using the topological properties [41-43]. Therefore, the most important donor-acceptor interactions predicted for the three tramadol species in both media by using the B3LYP/6-31G* method and the NBO program are shown in Table 7.

Table 7. Main delocalization energies (in kJ/mol) of free base, cationic, and hydrochloride species of Tramadol in the gas phase and aqueous solution by using B3LYP/6-31G* calculations.

Delocalization	B3LYP/6-31G*[a]					
	Free base		Cationic		Hydrochloride	
	Gas	Water	Gas	Water	Gas	Water
*LP(2)O2→ σ*C16-C18*	127.03	123.64			130.75	125.23
$\Delta E_{LP\rightarrow\sigma^*}$	**127.03**	**123.64**			**130.75**	**125.23**
*LP(2)O2→π*C12-C16*			63.91			
*LP(2)O2→π*C16-C18*				64.07		
$\Delta E_{LP\rightarrow\pi^*}$			**63.91**	**64.07**		
*π C11-C12→π*C13-C17*	71.14	71.39		33.98	70.39	70.14
*π C11-C12→π*C16-C18*	97.14	97.78		44.47	95.38	95.22
*π C11-C13→π*C17-C18*			46.89			
*π C12-C16→π*C11-C13*			50.36			
*πC13-C17→π*C11-C12*	93.54	94.25		49.11	94.21	95.59
*πC13-C17→π*C16-C18*	70.97	70.85		35.07	70.30	70.60
π C16-C18→π C11-C12*	68.88	68.88		37.36	69.84	70.26
πC16-C18→π C13-C17*	94.42	94.71		48.27	96.26	95.42
*π C16-C18→π*C11-C12*	1089.68	1172.57				
*πC16-C18→π*C13-C17*	1210.11					
*πC17-C18→π*C12-C16*			49.57			
$\Delta E_{\pi\rightarrow\pi^*}$	**2795.88**	**1670.43**	**146.82**	**248.26**	**496.38**	**497.23**
*σN3-C10→LP*H45*					43.97	58.23
*σN3-C14→LP*H45*					53.17	62.49
*σN3-C15→LP*H45*					54.17	58.64
$\Delta E_{\sigma\rightarrow LP^*}$					**151.31**	**179.36**
*LP(1)N3→LP*H45*					1277.53	1531.72
*LP(4)Cl46→LP*H45*					621.94	250.88
$\Delta E_{LP\rightarrow LP^*}$					**1899.47**	**1782.6**
ΔE_{TOTAL}	**2922.91**	**1794.07**	**210.73**	**312.33**	**2677.91**	**2584.42**

[a]This work

A detailed analysis of results reveals that the free base ($\Delta E_{LP\rightarrow\sigma^*}$ and $\Delta E_{\pi\rightarrow\pi^*}$) and the cationic species ($\Delta E_{LP\rightarrow\pi^*}$ and $\Delta E_{\pi\rightarrow\pi^*}$) in both media present two interactions while in the hydrochloride species four interactions are observed in both media ($\Delta E_{LP\rightarrow\sigma^*}$, $\Delta E_{\pi\rightarrow\pi^*}$, $\Delta E_{\sigma\rightarrow LP^*}$ and$\Delta E_{LP\rightarrow LP^*}$). The free base and hydrochloride species evidence lower stabilities in an aqueous solution, while the cationic one increases its stability in this medium, probably due to the positive charge on N3. Thus, the charged species justify their higher instability than the free base and hydrochloride ones with a total energy of 312.33 kJ/mol. On the other hand, the gas phase's the free base is most stable than the hydrochloride one in both media. The hydrochloride form is most stable in solution compared with the free base with a total energy of 2584.42 kJ/mol. The low stability in a solution of cationic species can probably be attributed to its hydration, as supported by the higher solvation energy or most negative value predicted for this species (-267.29 kJ/mol).

According to Bader's theory, the characteristic or nature of intra-molecular, H bonds, ionic, and/or covalent, polar interactions can be studied with the topological properties by using the AIM 2000 program of atoms in molecules [42,43]. Hence, the electron density, $\rho(r)$, the Laplacian values, $\nabla^2\rho(r)$, the eigenvalues $(\lambda1, \lambda2, \lambda3)$ of the Hessian matrix and, the $|\lambda1|/\lambda3$

ratio calculated in the bond critical points (BCPs) and ring critical points (RCPs) for the free base and cationic species of tramadol and the hydrochloride one in both media with the B3LYP/6-31G* method are shown in Tables 8 and 9, respectively.

Table 8. Analysis of the Bond Critical Points (BCPs) and Ring critical point (RCPs) for the free base and cationic species of Tramadol in the gas phase and aqueous solution by using the B3LYP/6-31G* method.

Free base								
Parameter[#]	**GAS PHASE**				**PCM**			
	H20---H37	RCPN1	RCP1	RCP2	H20---H37	RCPN1	RCP1	RCP2
ρ(r)	0.0094	0.0092	0.0200	0.0171	0.0099	0.0099	0.0199	0.0171
$\nabla^2\rho(r)$	0.0380	0.0428	0.1584	0.1084	0.0424	0.0452	0.1576	0.1080
λ1	-0.0092	-0.0077	-0.0147	-0.0136	-0.0087	-0.0081	-0.0147	-0.0136
λ2	-0.0039	0.0048	0.0816	0.0570	-0.0021	0.0023	0.0812	0.0571
λ3	0.0514	0.0459	0.0915	0.0651	0.0533	0.0510	0.0912	0.0647
|λ1|/λ3	0.1789	0.1677	0.1606	0.2089	0.1632	0.1588	0.1611	0.2102
Distances (Å)	2.162				2.178			
Cationic								
Parameter[#]	**GAS PHASE**				**PCM**			
	H22---H45	RCPN1	RCP1	RCP2	H22---H45	RCPN1	RCP1	RCP2
ρ(r)	0.0118	0.0113	0.0200	0.0170	0.0100	0.0100	0.0200	0.0170
$\nabla^2\rho(r)$	0.0480	0.0540	0.1576	0.1076	0.0420	0.0448	0.1580	0.1080
λ1	-0.0117	-0.0092	-0.0147	-0.0135	-0.0093	-0.0083	-0.0147	-0.0136
λ2	-0.0061	0.0077	0.0814	0.0575	-0.0029	0.0033	0.0815	0.0575
λ3	0.0660	0.0554	0.0912	0.0638	0.0546	0.0500	0.0913	0.0642
|λ1|/λ3	0.1772	0.1660	0.1611	0.2115	0.1703	0.1660	0.1610	0.2118
Distances (Å)	2.029				2.104			

[#]Parameters in a.u.

Table 9. Analysis of the Bond Critical Points (BCPs) and Ring critical point (RCPs) for the hydrochloride species of tramadol in the gas phase and aqueous solution by using the B3LYP/6-31G* method.

Hydrochloride							
GAS PHASE							
Parameter[#]	C12---H37	Cl46---H45	Cl46---H22	RCPN1	RCPN2	RCP1	RCP2
ρ(r)	0.0044	0.0696	0.0099	0.0061	0.0040	0.0200	0.0170
$\nabla^2\rho(r)$	0.0136	0.0968	0.0312	0.0252	0.0124	0.1580	0.1080
λ1	-0.0027	-0.1106	-0.0081	-0.0030	-0.0014	-0.0147	-0.0136
λ2	-0.0022	-0.1104	-0.0068	0.0059	0.0037	0.0815	0.0572
λ3	0.0187	0.3179	0.0463	0.0224	0.0105	0.0914	0.0645
|λ1|/λ3	0.1443	0.3479	0.1749	0.1339	0.1333	0.1608	0.2108
Distances (Å)	2.980	1.778	2.764				
PCM							
Parameter[#]	H20---H37	Cl46---H45	Cl46---H22	RCPN1	RCPN2	RCP1	RCP2
ρ(r)	0.0103	0.0376	0.0077	0.0069	0.0102	0.0200	0.0171
$\nabla^2\rho(r)$	0.0440	0.0732	0.0216	0.0244	0.0464	0.1576	0.1084
λ1	-0.0084	-0.0465	-0.0057	-0.0056	-0.0078	-0.0147	-0.0136
λ2	-0.0024	-0.0461	-0.0037	0.0014	0.0027	0.0814	0.0572
λ3	0.0549	0.1659	0.0313	0.0287	0.0518	0.0912	0.0648
|λ1|/λ3	0.1530	0.2802	0.1821	0.1951	0.1505	0.1611	0.2098
Distances (Å)	2.164	2.080	2.944				

[#]Parameters in a.u.

A new H bond with different involved atoms is observed in both media's free base and cationic species.

Thus, each C4-H20⋯H37 and N3-H45⋯H22 interaction of the free base and cationic species, respectively, form a new RCPN1 while the RCPs of R1 (3-methoxyphenyl) and R2 (cyclohexanol) rings are named RCP1 and RCP2, respectively. In the hydrochloride species, three different interactions are observed (C15-H37⋯C12, C6-H22⋯Cl46 and N3-H45⋯Cl46) in both media which one of them change in the solution. The molecular graphics of different interactions for the three tramadol species in the gas phase using the B3LYP/6-31G* method

are shown in Figure 8. The topological properties of R1 rings in the free base, cationic, and hydrochloride species are higher than the other ones (BCPs and RCPN1). Note that the distances between two involved atoms in H bonds are shorter in gas phase than in aqueous solution due to the hydration, except for the C4-H20···H37 interaction of hydrochloride form in a solution that presents a shorter distance different from that observed in the gas phase (C15-H37···C12). Thus, these studies show that the hydrochloride form in both media is the most stable species due to the three interactions that confer to its higher stability.

3.4. Frontier orbitals and global descriptors.

The low stability evidenced by NBO calculations for the cationic species of tramadol in aqueous solution is probably related to its most negative solvation energy value, while the hydrochloride species in this medium is the most stable in agreement with the studies observed from AIM calculations. Hence, it is impossible to understand why the hydrochloride species is a cationic one in this medium when its form shows high stability in the solution. Perhaps, an explanation could be obtained from frontier orbitals with the predictions of reactivities of three tramadol species in both media by using gap values, as suggested by Paar and Pearson [46] and, also with the predictions of its behaviors in both media [9,15,18-23].

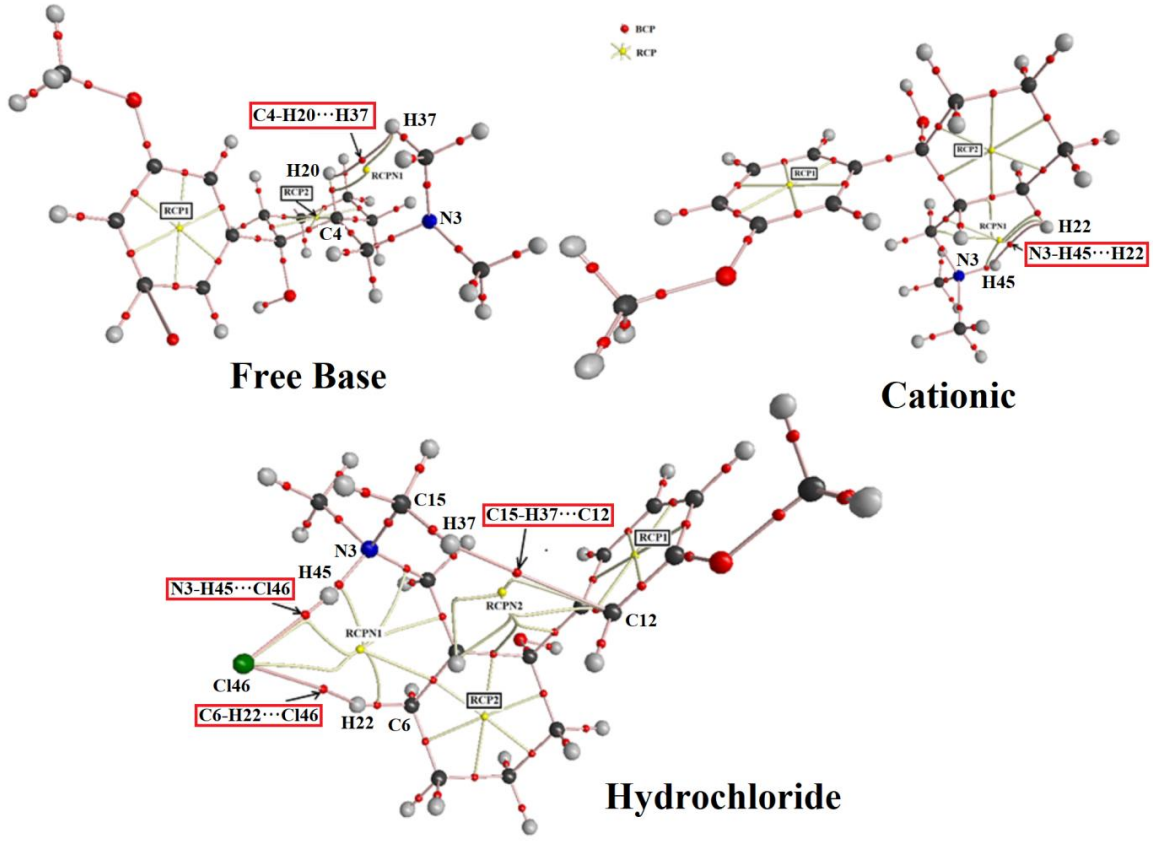

Figure 8. Molecular graphics of three species of tramadol in the gas phase showing their H bonds interactions by using the B3LYP/6-31G* method.

Thus, HOMO, LUMO, energy gaps and chemical potential (μ), electronegativity (χ), global hardness (η), global softness (S), global electrophilicity index (ω) and global nucleophilicity index (E) descriptors for the three species of tramadol in both media by using the B3LYP/6-31G* method are presented in Table 10 together with the corresponding equations [9,15,18-23].

Table 10. Frontier molecular HOMO and LUMO orbitals, gap and chemical potential (μ), electronegativity (χ), global hardness (η), global softness (S), global electrophilicity index (ω) and global nucleophilicity index (E) descriptors for the three species of Tramadol in the gas phase and aqueous solution by using the B3LYP/6-31G* level of theory.

B3LYP/6-31G*Method						
Orbital (eV)	Gas Phase			PCM		
	Free base	Cationic	Hydrochloride	Free base	Cationic	Hydrochloride
HOMO	-5.4201	-8.4813	-5.5243	-5.5398	-8.5026	-4.7987
LUMO	-0.0057	-3.0746	-0.4910	-0.0245	-3.1777	-0.6282
|GAP|	5.4144	5.4067	5.0332	5.5152	5.3250	4.1705
Descriptors						
(eV)	Free base	Cationic	Hydrochloride	Free base	Cationic	Hydrochloride
χ	-2.7072	-2.7034	-2.5166	-2.7576	-2.6625	-2.0853
μ	-2.7129	-5.7780	-3.0077	-2.7822	-5.8402	-2.7134
η	2.7072	2.7034	2.5166	2.7576	2.6625	2.0853
S	0.1847	0.1850	0.1987	0.1813	0.1878	0.2398
ω	1.3593	6.1747	1.7972	1.4035	6.4052	1.7654
E	-7.344	-15.620	-7.569	-7.672	-15.549	-5.658

[a]This work. $\chi = -[E(LUMO) - E(HOMO)]/2$; $\mu = [E(LUMO) + E(HOMO)]/2$; $\eta = [E(LUMO) - E(HOMO)]/2$; $S = ½\eta$; $\omega = \mu^2/2\eta$; $E = \mu x \eta$

The low gap value (4.1705 eV) of the hydrochloride species in solution reveals that this is the most reactive species in solution because its form has less negative E_{HOMO} (-4.7987 eV), as compared with the free base and cationic species. However, despite in the gas phase, the free base has less negative E_{HOMO} (-5.4201 eV); the hydrochloride form is also the most reactive species in this medium. Suppose now the hydrochloride forms of tramadol and antiviral amantadine are compared. In that case, it is observed that the species of an antiviral agent is most reactive (Egap= 4.1116 eV) than the corresponding to tramadol despite its most negative E_{HOMO} (-6.4736 eV) [23]. The cationic species of tramadol in both media are less reactive than the hydrochloride ones, probably due to the higher hydration, most negative solvation energy, and the high electrophilicity and nucleophilicity indexes predicted for this species in both media, as was also observed in the cationic species de amantadine [23]. These studies have evidenced that the hydrochloride species in both media are the most reactive in the two media while the free base species have higher gap values and, for these reasons, they are the less reactive in both media. Energetically, the hydrochloride species is the most stable one in solution due to higher stabilization E, as observed from NBO studies, while the AIM analyses for this species evidence higher number of interactions in solution, but one of these interactions change the character from covalent in the gas phase to ionic in solution, justifying this way the higher reactivity observed for this species in solution. Thus, the hydrochloride species is present in solution as cationic ones because the covalent character of the H45-Cl46 bond slightly changes to ionic (N3-H45⋯ Cl46) in this medium, as revealed by bond orders studies. In the hydrochloride species of antiviral amantadine, a similar resulted was observed [23].

3.5. Vibrational study.

Optimizations of tramadol species in both media using hybrid B3LYP/6-31G* calculations have shown C_1 symmetries for the three forms. The numbers of normal vibration modes expected for a free base, cationic, and hydrochloride forms of tramadol are 126, 129, and 132. All modes present activity in both infrared and Raman spectra. Experimental Attenuated Total Reflectance Infrared (ATR-IR) and Raman spectra of hydrochloride form of tramadol available from the literature can be seen in Figures 9 and 10 compared with the corresponding predicted for the three species by using the B3LYP/6-31G* method [48]. Better

correlations were obtained when the Raman spectra were corrected from activities to intensities using well-known equations [39,40]. The harmonic force fields for those three species were calculated using the scaled quantum mechanical force field (SQMFF) methodology using normal internal coordinates and the Molvib program [27-29].

Scaling factors were employed in this procedure together with potential energy distribution (PED) contributions ≥ 10 % [28]. In Table 11 are presented observed and calculated wavenumbers for the three species of tramadol. Comparing and analyzing all spectraall spectra exhaustively, we observed that the intense IR band predicted the hydrochloride species at 1944 cm-1 using B3LYP/6-31G* calculations observed with lower intensity in the Raman spectrum, are not observed in both experimental spectra.

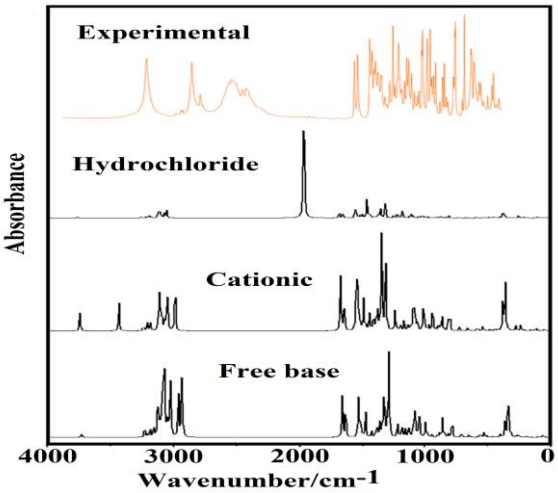

Figure 9. Experimental ATR-IR spectra of hydrochloride species of tramadol in solid phase [48] compared with the predicted for the three species in the gas phase by using the hybrid B3LYP/6-31G* method.

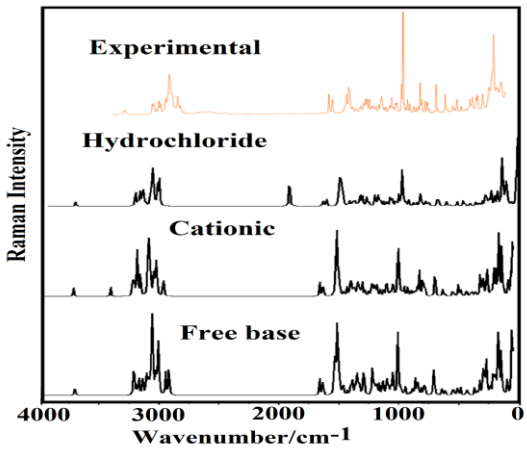

Figure 10. Experimental Raman spectra of hydrochloride species of tramadol in solid phase [48] compared with the predicted for the three species in the gas phase by using the hybrid B3LYP/6-31G* method.

Table 11. Observed and calculated wavenumbers (cm^{-1}) and assignments of free base, cationic, and hydrochloride species of Tramadol in the gas phase.

Experimental		B3LYP/6-31G* Method[a]					
		Hydrochhhloride		Cationic		Free base	
ATR[c]	Raman[c]	SQM[b]	Assignments[a]	SQM[b]	Assignments[a]	SQM[b]	Assignments[a]
3403sh		3573	νO1-H31	3580	νO1-H31	3570	νO1-H31
3304s	3297w			3283	νN3-H45		
3109sh	3204vw	3096	νC18-H41	3102	νC18-H41	3095	νC18-H41
	3153vw	3091	νC13-H33	3092	νC13-H33	3092	νC13-H33
3067vw	3068w	3073	νC12-H32	3079	ν_aCH_3(C15)	3074	νC12-H32
	3059w	3062	ν_aCH_3(C15)	3068	νC12-H32	3054	νC17-H40
3052vw	3049sh	3056	νC17-H40	3068	ν_aCH_3(C14)	3025	ν_aCH_3(C19)
		3054	ν_aCH_3(C14)	3066	νC17-H40	2997	ν_aCH_3(C15)
		3040	ν_aCH_3(C15)	3065	ν_aCH_3(C15)	2990	ν_aCH_3(C14)
		3036	ν_aCH_3(C14)	3062	ν_aCH_3(C14)	2980	ν_aCH_2(6)
3019vw	3030w	3031	ν_aCH_3(C19)	3044	ν_aCH_2(10)	2971	ν_aCH_2(10)
3003vw	3013w	3013	ν_aCH_2(10)	3042	ν_aCH_3(C19)	2961	ν_aCH_2(9)
2979sh	2997w	2976	ν_aCH_2(6)	2986	ν_sCH_2(10)	2954	ν_aCH_3(C15), ν_sCH_3(C15)
	2975sh	2966	ν_sCH_2(10)	2980	ν_aCH_2(9)	2954	ν_aCH_3(C19)
		2965	ν_aCH_2(7)	2977	ν_sCH_3(C15)	2946	ν_aCH_2(7)
		2959	ν_aCH_3(C19)	2976	ν_aCH_3(C19)	2945	ν_aCH_3(C14)
	2956w	2956	ν_sCH_3(C15)	2971	ν_aCH_2(8)	2943	ν_aCH_2(8)
		2956	ν_aCH_2(8)	2971	ν_sCH_3(C14)	2926	ν_sCH_2(6)
		2950	ν_sCH_3(C14)	2963	ν_aCH_2(7)		
2940sh		2949	ν_aCH_2(9)	2952	ν_aCH_2(6)		
2931s	2937sh	2937	νC4-H20	2935	ν_sCH_2(9)	2918	ν_sCH_2(9)
	2925s	2920	ν_sCH_2(9)	2932	νC4-H20	2903	νC4-H20
2912sh		2917	ν_sCH_2(6)	2924	ν_sCH_2(7)	2899	ν_sCH_3(C19)
	2904sh	2908	ν_sCH_2(8)	2913	ν_sCH_3(C19)	2898	ν_sCH_2(7)
2863w	2863sh	2902	ν_sCH_3(C19)	2909	ν_sCH_2(8)	2890	ν_sCH_2(8)

Experimental		B3LYP/6-31G* Method[a]					
		Hydrochhhloride		Cationic		Free base	
2842w	2854m	2901	ν_sCH_2(7)	2856	ν_sCH_2(6)	2839	ν_sCH_2(10)
	2836w	1868	νN3-H45			2813	ν_aCH_3(C15), ν_sCH_3(C15)
	2809w					2805	ν_sCH_3(C14)
1608s	1606s	1609	νC12-C16,νC13-C17 νC11-C12,νC17-C18	1609	νC12-C16,νC11-C12 νC13-C17,νC17-C18	1611	νC12-C16,νC13-C17 νC11-C12,νC17-C18
1582s	1577s	1583	νC16-C18νC11-C13	1583	νC16-C18,νC11-C13	1584	νC16-C18,νC11-C13
1484vs		1489	βC12-H32	1491	βC12-H32	1489	βC17-H40,βC12-H32
1484vs		1481	δ_aCH_3(C15)ρ'N3-H45	1475	δ_aCH_3(C15)	1477	δ_aCH_3(C14),δ_aCH_3(C15)
						1471	δ_aCH_3(C19)
		1470	δ_aCH_3(C19)	1467	δ_aCH_3(C19)	1470	δCH_2(C10)
1464s	1461s	1466	δCH_2(C10) δ_aCH_3(C14)	1465	δ_aCH_3(C14)	1466	δCH_2(C9), δCH_2(C6)
		1463	δCH_2(C9)δCH_2(C8)	1463	δ_aCH_3(C15),δ_aCH_3(C14)	1464	δ_aCH_3(C15)
		1462	δ_aCH_3(C15)	1460	δCH_2(C8)	1455	δ_aCH_3(C19),δCH_2(C10)
		1458	δCH_2(C10) δ_aCH_3(C15)	1456	δCH_2(C10)	1454	δ_aCH_3(C19)
		1455	δ_aCH_3(C19)	1456	δ_aCH_3(C19)	1453	δCH_2(C8)
		1452	δCH_2(C8) δCH_2(C6)	1450	δCH_2(C9)	1449	δ_aCH_3(C14)
1449s	1446sh	1447	δCH_2(C9)	1444	δCH_2(C7)	1447	δCH_2(C9), δCH_2(C6)
		1444	δ_aCH_3(C14)	1441	δ_sCH_3(C19) νC11-C12	1442	δCH_2(C7)
		1444	δCH_2(C7)	1441	δCH_2(C7), δCH_2(C6)	1441	δCH_2(C7), δ_sCH_3(C19)
		1440	δ_sCH_3(C19) νC11-C12	1439	δCH_2(C6)		
1435s	1439s	1439	δCH_2(C10)ρ'N3-H45	1430	δ_sCH_3(C19), βC18-H41	1433	δ_sCH_3(C15) δ_sCH_3(C14)
1431sh	1430sh	1430	δ_sCH_3(C19) βC18-H41	1425	δ_sCH_3(C14) δ_sCH_3(C15)	1431	δ_sCH_3(C19) βC18-H41
1416s	1411w	1425	ρN3-H45	1413	ρ'N3-H45,ρN3-H45		
	1401sh	1406	wagCH_2(C10)	1401	δ_sCH_3(C15)	1407	δ_sCH_3(C15) wagCH_2(C10)
1389m	1389sh	1394	δ_sCH_3(C14)	1396	δ_sCH_3(C14)	1399	δ_sCH_3(C14)
		1390	wagCH_2(C6)	1386	wagCH_2(C8)	1377	wagCH_2(C9)
		1390	δ_sCH_3(C15)	1376	wagCH_2(C7),wagCH_2(C8)	1375	wagCH_2(C8),wagCH_2(C7)
	1383w	1379	wagCH_2(C8)	1372	wagCH_2(C9),wagCH_2(C10)	1368	wagCH_2(C7)
		1372	wagCH_2(C9)	1372	wagCH_2(C6)ρ'C4-H20	1362	wagCH_2(C8)
1361w		1363	wagCH_2(C7)	1363	wagCH_2(C7)		
1342w	1342w	1338	ρCH_2(C10), ρC4-H20	1332	ρC4-H20	1341	ρCH_2(C10)
1319m	1318w	1322	νC13-C17,νC12-C16	1322	νC13-C17	1324	ρC4-H20
		1316	ρ'C4-H20	1318	ρC4-H20	1319	νC13-C17
		1311	ρCH_2(C7),ρCH_2(C6)	1306	ρCH_2(C7)	1306	ρCH_2(C7)
	1301m	1300	ρCH_2(C10)	1298	νC16-O2	1294	νC16-O2,βC12-H32
1293vs	1287m	1293	ρCH_2(C10)	1288	ρCH_2(C10)	1292	ρ'C4-H20
1276w	1271m					1274	ρ'CH_3(C14), νN3-C10
1258sh	1253sh	1263	ρC4-H20, ρCH_2(C9)	1265	ρCH_2(C9),ρCH_2(C6)	1260	ρCH_2(C9),ρCH_2(C6)
1247s	1242w	1259	νC16-O2	1265	νC16-O2	1255	νC16-O2
		1244	ρ'CH_3(C14)	1240	ρCH_2(C8)	1243	ρCH_2(C8)
1223w	1235sh	1237	ρCH_2(C8) ρ'CH_3(C15)	1220	ρ'CH_3(C15),ρ'CH_3(C14)		
1199m	1218w	1199	δC5O1H31	1195	δC5O1H31	1193	ρCH_2(C9)
1181s	1192w	1190	ρCH_3(C19)	1189	ρCH_3(C19)	1190	ρCH_3(C19)
1166s	1173sh	1174	βC17-H40,βC13-H33	1176	βC17-H40,βC13-H33	1176	δC5O1H31
		1173	ρCH_3(C14) ρCH_3(C15)	1174	ρCH_2(C9)	1173	βC13-H33
	1168s	1162	νC5-C11	1158	νC5-C11	1165	ρCH_3(C14), ρCH_3(C15)
1140m	1160sh	1154	ρ'CH_3(C19)	1151	ρ'CH_3(C19)	1155	νC5-C11
	1148w	1154	νC5-C11	1146	ρ'CH_3(C15)	1154	ρ'CH_3(C19)
1118w	1134w	1126	ρCH_2(C8)	1120	ρCH_2(C8)	1129	ρCH_2(C6),ρCH_2(C9)
1112sh	1109w	1102	νC13-C17			1105	ρCH_3(C14), ρCH_3(C15)
	1101sh			1099	νC13-C17,νC17-C18	1099	νC17-C18
1092w	1087s	1085	νC5-O1	1083	νC5-O1	1083	νC5-O1
1077w	1073w	1071	νC4-C10,νC4-C6	1070	νC4-C10	1071	νC4-C10
1056s	1053m	1062	νC7-C9,νC6-C8	1060	νC7-C9,νC5-C7	1060	νC7-C9
1056s	1053m	1058	ρCH_3(C14) ρCH_3(C15)			1054	νC19-O2
1048vs	1044m	1053	νC19-O2	1045	νC19-O2	1049	νC4-C10,νC6-C8
1048vs	1044m	1046	νC4-C10	1036	ρCH_3(C14)	1040	ρ'CH_3(C14),νN3-C15 ρ'CH_3(C15),νN3-C14
1013s	1006vs	1023	νC5-C4,νC5-C7	1030	ρCH_3(C15)	1021	νC5-C4,νC5-C7
987vs	991vs	1002	νN3-C14,νN3-C15	1014	νC5-C4	1014	νN3-C10
987vs	982sh	992	βR_1(A1)	991	βR_1(A1)	993	βR_1(A1)
				974	γC17-H40		
976m	970w	976	νN3-C10,βR_1(A2)	971	νN3-C15	965	γC17-H40,γC13-H33
960m		967	γC17-H40,γC13-H33	964	νC7-C9,νC5-O1	964	νC5-O1
		964	γC17-H40νC6-C8	959	νC6-C8	960	νC6-C8
943s	954s	951	νN3-C10	929	νC5-O1	930	νC5-O1
908w	937m	932	νC5-O1	907	νN3-C14		
	902w	899	τwCH_2(C6)	895	νN3-C10	900	τwCH_2(C6), τwCH_2(C7)

Experimental		B3LYP/6-31G* Method[a]					
		Hydrochhhloride		Cationic		Free base	
886m	882w	888	γC12-H32,γC18-H41	891	γC18-H41,γC13-H33	885	γC18-H41
872s		881	γC12-H32	874	γC12-H32	879	γC12-H32
853w	866w	867	τwCH$_2$(C10)	844	νC8-C9	852	νN3-C15,νN3-C14
842w	849s	839	νC8-C9	835	τwCH$_2$(C9), νC8-C9	838	νC8-C9
812sh	837s	825	βR$_3$(A1)	822	τwCH$_2$(C10)	823	τwCH$_2$(C10) τwCH$_2$(C8)
798m	809m	813	τwCH$_2$(C10) τwCH$_2$(C8)	801	νN3-C15,νN3-C10	820	νN3-C15
785s	792m	789	γC18-H41	794	γC18-H41,γC13-H33	787	γC18-H41γC17-H40
783vs	777w	772	νC4-C6,τwCH$_2$(C8)	764	νC4-C6,τwCH$_2$(C8)	770	νC4-C6
765sh	754vw	750	τwCH$_2$(C7) τwCH$_2$(C9)	742	τwCH$_2$(C7),τwCH$_2$(C9) τwCH$_2$(C6)	745	τwCH$_2$(C7) τwCH$_2$(C9),τwCH$_2$(C6)
724w	718s	702	τR$_1$(A1)	697	τR$_1$(A1)	700	βR$_2$(A1),τwCH$_2$(C6)
706vs	703vw	698	γC11-C5	691	βR$_2$(A1),νC5-C4	697	τR$_1$(A1)
650s	644s	650	βR$_2$(A1)	643	βR$_2$(A1)	649	βR$_2$(A1)
625s	624w	625	τR$_2$(A1), γC16-O2	624	γC16-O2	624	γC16-O2
586m	582w	574	δC16O2C19,βC16-O2	574	δC16O2C19,βC16-O2	574	δC16O2C19,βC16-O2
572m	568w	566	δC14N3C10, ρC5-O1	555	δC10C4C5, δC14N3C10	556	ρC5-O1, δC14N3C10
551w	548s	527	βR$_2$(A2)	526	βR$_2$(A2)	533	βR$_2$(A2)
516w	512w	510	βR$_3$(A1)	507	βR$_3$(A1)	509	βR$_3$(A1)
481w	477w	474	βR$_1$(A2)	466	βR$_1$(A2)	466	βR$_1$(A2)
470m	465vw	465	τR$_3$(A1)	462	τR$_3$(A1)	462	τR$_3$(A1)
444w	439s	437	δC14N3C15	440	δC15N3C10	453	δC14N3C15
423w	420s	428	δC15N3C10	430	δC14N3C15	406	βR$_2$(A2)
416sh	389s	406	δC15N3C10	403	δC15N3C10,βR$_2$(A2)	390	δC15N3C10
	377s	384	δC14N3C10	366	δC7C5C11	370	δC7C5C11
	366sh	360	δC10C4C6,δC7C5C11	355	δC10C4C6	350	δC10C4C6
	337s	337	τR$_1$(A2)	328	ρ'C5-O1	331	ρ'C5-O1
	325sh	332	ρ'C5-O1	322	τR$_1$(A2)	326	δC14N3C10
	320sh	315	τO1-H31	311	τO1-H31	310	τO1-H31
	308vw	296	βR$_3$(A2)	288	βR$_3$(A2)	293	βR$_3$(A2)
	280s	277	ρC5-O1	268	ρC5-O1	269	ρC5-O1
	256sh	257	τR$_2$(A1), τwCH$_3$(C19)			258	τwCH$_3$(C19)
	256sh			253	τR$_2$(A1), τR$_3$(A1)	250	τwCH$_3$(C14),δC16O2C19
	244vs	243	δC4C5C11	244	τR$_2$(A1), τwCH$_3$(C19)	235	τwCH$_3$(C14)
	237sh	238	δC10C4C5			231	τwCH$_3$(C14)
	225sh	227	νH45-Cl46	228	δC4C10N3,τR$_1$(A1)	224	τwCH$_3$(C15)
	218w	211	τR$_3$(A2)	215	τwCH$_3$(C14), τwCH$_3$(C15)	199	τR$_2$(A1)
	191sh	199	τwCH$_3$(C19)	193	τR$_3$(A2)	194	τR$_3$(A2),τR$_2$(A2)
	186s	193	τwCH$_3$(C15)	192	τR$_2$(A1), τwCH$_3$(C19)		
	174sh	182	τwCH$_3$(C14)	184	τR$_2$(A2)		
	165sh	166	βC11-C5, δC4C10N3	146	βC11-C5	155	βC11-C5
		118	τwCH$_3$(C15)	120	δC4C10N3	113	δC10C4C5, δC4C10N3
		107	τN3-H45				
		97	τO2-C16,τC10-C4	99	τO2-C16,τwCH$_3$(C19)	101	τO2-C16,τwCH$_3$(C19)
		90	τR$_2$(A2)				
				76	δC4C5C11	75	δC4C5C11
		69	τO2-C16	72	τO2-C16	68	τO2-C16
		59	δN3H45Cl46	45	τN3-C10,γC11-C5	45	τC5-C11,γC11-C5
		34	τC5-C11	37	τC10-C4	32	τN3-C10
		31	τN3-C10	27	τC5-C11	26	τC10-C4
		16	τC10-C4,τN3-C10				

Abbreviations: ν, stretching; β, deformation in the plane; γ, deformation out of plane; wag, wagging; τ, torsion; β$_R$, deformation ring τ$_R$, torsion ring; ρ, rocking; τw, twisting; δ, deformation; a, antisymmetric; s, symmetric; (A$_1$), Ring 1; (A$_2$), Ring 2. [a]This work, [b]From scaled quantum mechanics force field, [c]From Ref [48].

For these reasons, the hydrochloride form of tramadol is a cationic one in the solid phase, in agreement with all studied hydrochloride species of different pharmacological drugs by using vibrational spectroscopy [3-5,7,9-23]. That strong IR band calculated at 1944 cm^{-1} is predicted by SQM calculations at 1868 cm$^{-1.}$ It is assigned to the νN3-H45 stretching mode of hydrochloride form.

Probably, the numerous IR bands observed in the 1700-400 cm^{-1} region in the ATR spectrum could indicate the presence of a free base in the solid phase. Obviously, the differences observed between experimental and theoretical spectra can be attributed to the calculations. These were performed in the gas phase, where the packing forces existent in the

solid phase were not considered. Thus, the group of bands between 2758 and 2368 cm^{-1}, centered in the IR spectrum at 2605 cm^{-1} and 2621 cm^{-1} in the Raman one, could be associated with dimeric species not considered in this work. Brief discussions of some assignments are presented below.

3.5.1. Band Assignments.

4000-2000 cm^{-1} region. In this region are expected characteristic bands related to stretching modes of OH, NH, CH_3, CH_2, and aromatic and aliphatic C-H groups [3-5,7,9-23]. The OH stretching modes in the three species are predicted in the same regions; hence, the shoulder at 3403 cm^{-1} is assigned to these stretching modes. The strong IR band at 3304 cm^{-1} is quickly assigned to NH stretching of cationic species. The aromatic CH stretching mode is assigned as predicted by calculations between 3102 and 3054 cm^{-1}, while the only aliphatic mode in the three species is assigned between 2937 and 2903 cm^{-1}. The antisymmetric and symmetric modes of CH_3 groups are assigned from 3068 cm^{-1} up to 2805 cm^{-1}, while these modes for CH_2 groups between 3044 and 2839 cm^{-1}, as detailed in Table 11 and, as observed in similar compounds [3-5,7,9-23]. The group of bands between 2758 and 2368 cm^{-1} can be attributed to dimeric hydrochloride species, as reported for anti-hypertensive agent tolazoline hydrochloride [18,19].

1800-1000 cm^{-1} region. Characteristic bands associated with deformation, wagging, and rocking modes of CH_2, CH_3, OH, NH and C-H groups and C-C, N-C, and C-O stretching modes are expected in this region [3-5,7,9-23]. The strong pairs of IR/Raman band at 1608/1582, and 1606/1577 cm^{-1} are assigned to C=C stretching modes of R1 rings, while the very strong IR band at 1484 cm^{-1} is associated with in-plane CH deformations of three species. The three antisymmetric and symmetric CH_3 deformations and CH_2 deformations modes are assigned between 1481 cm^{-1} and 1390 cm^{-1}, while the IR bands at 1199 and 1166 cm^{-1} are assigned to OH deformations, as predicted by SQM calculations. The strong IR band at 1416 cm^{-1} is assigned to N-H rocking modes of cationic and hydrochloride species, while the band of medium intensity at 1319 cm^{-1} and the intense IR band at 1247 cm^{-1} are assigned to C-C and C16-O2 stretching modes, respectively. The intense Raman band at 1087 cm^{-1} can be assigned to C5-O1 stretching modes of three tramadol species, while other C-C stretching modes can also be assigned to IR and Raman bands between 1077 and 987 cm^{-1}.

1000-10 cm^{-1} region. In this region, the SQM calculations predict C-C, N-C, and C-O stretching, OH, CH_3, and CH_2 twisting and skeletal modes of both rings. The strong band at 783 cm^{-1} is assigned to C4-C6 stretching modes of the three species because the SQM calculations predict these modes between 772 and 764 cm^{-1} while the intense band located at 987 cm^{-1} is associated with one of three deformations rings R1 of three species (βR_1(A1)). The IR at 798 cm^{-1} can be assigned to stretching modes of N3-C15 and N3-C10 bonds or the twisting mode of CH_2 groups, while the strong Raman bands at 389, 377, and 280 cm^{-1} are associated with C15N3C10, C14N3C10, C7C5C11 deformations, and C5-O1 rocking modes.

Deformations and torsions of methoxyphenyl rings (R1 or A1) and cyclohexanol (R2 or A2) are predicted by SQM calculations in the 1000-60 cm^{-1} region, as was observed in species containing six members rings [3-5,7,9-23]. Note that practically in all regions, the SQM calculations predict some vibration modes' coupling, as was detailed in Table 11.

3.6. Force constants.

The determinations of harmonic force fields for the three tramadol species in both media with the SQMFF methodology and Molvib program by using the B3LYP/6-31G* level of the theory have allowed computing scaled force constants for those species in the two media [27-29]. The results for the three species of tramadol in both media are presented in Table 12.

Table 12. Scaled internal force constants for the free base, cationic, and hydrochloride tramadol species in gas and aqueous solution phases using the B3LYP/6-31G* method.

Force constant	B3LYP/6-31G* method					
	Tramadol[a]					
	Free base		**Cationic**		**Hydrochloride**	
	Gas	PCM	Gas	PCM	Gas	PCM
f(νO-H)	7.13	7.09	7.17	7.09	7.14	7.11
f(νN-H)			5.98	6.03	2.82	4.78
$f(\nu C\text{-}O)_{OH}$	4.48	4.33	4.57	4.41	4.52	4.41
$f(\nu C\text{-}O)_{OCH3}$	5.45	5.05	5.50	5.05	5.48	5.03
f(νC-N)	4.72	4.59	3.86	4.04	4.27	4.13
$f(\nu C\text{-}H)_{R1}$	5.21	5.23	5.21	5.23	5.21	5.23
$f(\nu C\text{-}H)_{R2}$	4.66	4.75	4.76	4.83	4.76	4.82
$f(\nu C\text{-}C)_{R}$	6.45	6.43	6.43	6.43	6.43	6.43
$f(\nu CH_2)$	4.73	4.73	4.80	4.81	4.79	4.80
$f(\nu CH_3)$	4.75	4.80	5.02	5.04	4.96	5.03
$f(\delta CH_2)$	0.75	0.74	0.74	0.73	0.75	0.73
$f(\delta CH_3)$	0.58	0.57	0.57	0.56	0.57	0.56

Units are mdyn $Å^{-1}$ for stretching and mdyn Å rad^{-2} for angle deformations. [a]This work.

The *f(νO-H)* force constants of the three species show a decrease in solution due to the hydrations of these groups with water molecules, as also was observed in the $f(\nu C\text{-}O)_{OH}$ and $f(\nu C\text{-}O)_{OCH3}$ force constants. However, the *f(νN-H)* force constants of hydrochloride species increase in solution while remains practically constant in the cationic species. In the hydrochloride form, the presence of Cl atom justifies that observation because the N3-H45 bond is shortened of 1.128 Å in the gas phase to 1.056 Å in solution while the H45⋯Cl46 bond increases from 1.778 Å in the gas phase to 2.080 Å in solution. The remaining force constants do not show changes in the three species or with the medium and show values approximately similar to reported for other pharmacological species [3-5,7,9-23].

3.7. NMR study.

The GIAO method was used to predict the ^{1}H and ^{13}C NMR chemical shifts of three species of tramadol in an aqueous solution with the hybrid B3LYP/6-31G* level of theory [47]. These results were compared with the corresponding experimental spectra available from the literature for tramadol hydrochloride solution in DMSO-d6 [24]. Comparisons between experimental and theoretical ^{1}H and ^{13}C NMR chemical shifts are presented in Tables 13 and 14, respectively, using the RMSDs values [24].

Table 13. Observed and calculated ^{1}H chemical shifts (δ in ppm) for the three Tramadol species in aqueous solution by using the B3LYP/6-31G* method.

Tramadol[a]							
H atom	**Base**		**Cationic**		**Hydrochloride**		**Exp[b]**
	Gas	**PCM**	**Gas**	**PCM**	**Gas**	**PCM**	
20-H	2.37	2.49	2.61	1.89	1.80	2.30	2.27
21-H	2.22	2.29	2.47	1.78	1.38	2.37	2.22
22-H	2.67	2.46	1.54	0.71	3.00	3.28	2.27
23-H	2.49	2.45	2.67	1.93	1.83	2.43	2.22

Tramadol[a]							
H atom	Base		Cationic		Hydrochloride		Exp[b]
	Gas	PCM	Gas	PCM	Gas	PCM	
24-H	1.66	1.64	2.12	1.38	0.98	1.74	2.27
25-H	2.20	2.22	2.57	1.90	1.47	2.46	2.22
26-H	1.91	1.89	2.13	1.38	1.49	1.84	2.27
27-H	1.86	1.83	2.24	1.54	1.19	1.90	2.22
28-H	2.41	2.39	2.56	1.87	1.62	2.42	2.27
29-H	2.87	3.04	3.98	3.05	2.03	3.43	2.81
30-H	2.24	1.92	3.25	2.45	2.24	2.38	2.55
31-H	0.32	0.43	1.14	0.46	0.33	0.64	5.12
32-H	6.98	7.00	6.91	6.17	6.37	6.95	7.09
33-H	7.34	7.27	7.21	6.52	6.55	7.22	7.07
34-H	2.57	2.50	3.29	2.56	1.85	2.80	2.41
35-H	2.30	1.90	3.13	2.39	1.35	1.90	2.41
36-H	2.53	2.48	3.29	2.55	2.08	3.20	2.41
37-H	2.72	2.78	3.50	2.86	1.70	3.08	2.55
38-H	2.30	2.31	3.07	2.33	1.99	2.83	2.55
39-H	1.66	1.50	2.63	1.93	0.54	1.70	2.55
40-H	7.50	7.49	7.81	7.12	6.81	7.57	7.28
41-H	6.70	6.72	7.09	6.43	6.05	6.80	7.07
42-H	4.27	4.27	4.53	3.82	3.64	4.33	3.76
43-H	3.95	3.97	4.07	3.31	3.21	3.87	3.76
44-H	3.93	3.89	4.08	3.37	3.23	4.01	3.76
RMSD	**1.01**	**1.00**	**0.96**	**1.08**	**1.24**	**0.99**	

[a]This work GIAO/B3LYP/6-31G* Ref. to TMS, [b]From Ref [24].

In this study, the values in the gas phase were also included in the tables. Analyzing the RMSDs for the ^{1}H nucleus of all species, we observed that in good general correlations are observed for the three species with values between 1.24 and 0.96 ppm and, in particular, the hydrochloride species in solution shows a low value because it is the compared species. The free base values in both media, closer than the corresponding cationic species, suggest that the free base could be protonated in solution. Suppose now the results for the 13C nucleus are compared. In that case, it is observed that the free base and hydrochloride species present similar correlations in the RMSDs (9.96-9.54 ppm), while lower concordances are observed in the cationic species in both media (10.36-10.03 ppm). Such differences could be associated with the different media recorded and calculated the spectra and calculations because better correlations are observed when the species are optimized using the B3LYP/6-311++G** method and, especially, the chemical shifts for the ^{1}H nucleus.

Table 14. Observed and calculated ^{13}C chemical shifts (δ in ppm) for the three Tramadol species in aqueous solution by using the B3LYP/6-31G* method.

Tramadol[a]							
C atoms	Base		Cationic		Hydrochloride		Exp[b]
	Gas	PCM	Gas	PCM	Gas	PCM	
4-C	38.4	37.8	36.6	35.8	36.8	36.8	40.21
5-C	69.3	69.8	68.7	69.4	69.7	69.7	73.87
6-C	20.6	19.6	18.4	18.1	23.4	19.6	26.16
7-C	36.7	37.4	34.1	36.2	35.7	36.9	40.39
8-C	20.4	20.2	18.6	18.7	19.2	19.1	24.47
9-C	17.1	16.7	15.2	15.4	16.5	16.2	21.16
10-C	50.6	51.7	56.6	55.5	52.4	51.4	59.33
11-C	136.7	137.3	129.7	130.5	136.0	135.6	150.0
12-C	100.7	100.8	99.3	98.9	101.0	100.1	111.52
13-C	103.1	102.9	100.7	101.3	102.9	102.5	117.22
14-C	39.2	40.1	37.5	37.9	35.5	37.6	44.77
15-C	33.8	34.5	32.8	32.7	32.0	30.7	40.60
16-C	143.8	144.6	145.6	146.3	144.4	144.9	159.1
17-C	114.9	115.3	117.7	118.0	115.5	116.1	129.06

Tramadol[a]							
C atoms	Base		Cationic		Hydrochloride		Exp[b]
	Gas	PCM	Gas	PCM	Gas	PCM	
18-C	94.5	94.9	98.4	99.0	95.3	95.9	111.12
19-C	45.1	45.8	45.9	46.4	45.1	45.9	54.96
RMSD	9.86	9.54	10.36	10.03	9.92	9.96	

[a]This work GIAO/B3LYP/6-31G* Ref. to TMS, [b]From Ref [24].

3.8. Electronic spectrum.

The electronic spectra for the three tramadol species were also predicted in an aqueous solution because tramadol hydrochloride is freely soluble in water, as reported in the literature [24]. These theoretical spectra were obtained using the Time-dependent DFT calculations (TD-DFT) with the Gaussian program and the B3LYP/6-31G* method [35]. The experimental spectrum was recorded for tramadol hydrochloride in methanol from 200 to 400 nm [24]. All spectra are compared in Figure 11. It is possible to observe that the experimental UV spectrum shows absorption maxima at 217 nm and 272 nm while the predicted spectrum for the free base present maxima at 180 and 245 nm and a shoulder at 212 nm. In the cationic species, only two maxima are observed at 212 and 250 nm. In the UV spectrum of hydrochloride form, they are observed two maxima at 245 and 290 nm.

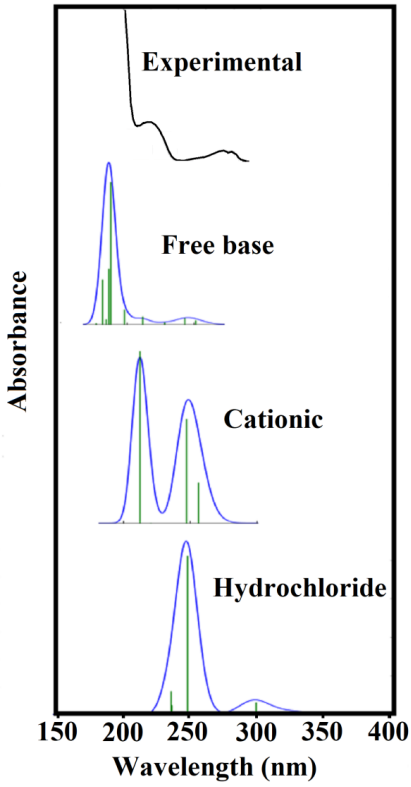

Figure 11. Experimental electronic spectrum of hydrochloride tramadol in methanol [24] compared with the corresponding predicted for the three species in aqueous solution using the B3LYP/6-31G* method.

These results show that part of the free base is protonated in solution because the shoulder and the maximum respectively at 212 and 245 nm correspond to bands of cation while part of hydrochloride species is as cationic one because the two experimental bands at 217 nm and 272 nm are in agreement with a band of the cation (212 nm) and other of free base protonated (290 nm). The band at 180 nm observed for the free base cannot be seen experimentally because the experimental spectrum was recorded between 200 and 400 nm. These studies show that the three species can be present in a solution of hydrochloride tramadol

and that the bands can be attributed to $\pi \rightarrow \pi^*$ transitions due to the C=C double bonds, as predicted by the NBO analysis and in agreement with literature data [49,50].

4. Conclusions

In this research, three species of narcotic tramadol agent's theoretical structures were studied in the gas phase and aqueous solution by using the functional hybrid B3LYP with the 6-31G* basis set. Comparisons of predicted infrared, Raman, ^{1}H, and ^{13}C NMR and electronic spectra for the free base, cationic, and hydrochloride species of tramadol with the corresponding experimental ones have evidenced reasonable correlations for the cationic species showing that this species present in the solid phase and in solution. The vibrational studies have revealed that the species cationic is present in the solid phase because the most intense band predicted for the hydrochloride in infrared and Raman spectra is not observed in the experimental spectra. The harmonic force fields, together with the normal internal coordinates and scaling factors, have allowed the complete vibrational assignments of 126, 129, and 132 vibration modes expected for a free base, cationic, and hydrochloride species, respectively, by using the SQMFF methodology. The cationic species evidence the most negative solvation energy and higher hydration in solution in agreement with its lower stability, while the hydrochloride species is the most reactive in solution. MK charges and NBO and AIM studies support cationic species' instability due to the positive charge on N atom. Comparisons of the experimental UV spectrum of hydrochloride tramadol with the predicted for the three species suggest that the free base, cationic, and hydrochloride species can be present in solution.

Funding

This research received no external funding.

Acknowledgments

This work was supported with grants from CIUNT Project Nº 26/D608 (Consejo de Investigaciones, Universidad Nacional de Tucumán). The author would like to thank Prof. Tom Sundius for his permission to use MOLVIB.

Conflicts of Interest

The authors declare no conflict of interest.

References

1. Veber. D.F.; Johnson, S.R.; Cheng, H.-Y; Brian, R.; Ward, K.W.; Kopple, K.D. Molecular Properties that influence the oral bioavailability of drug candidates. *J. Med. Chem*. **2002**, *45*, 2615-2623, https://doi.org/10.1021/jm020017n.
2. Lipinski, C.A.; Lombardo, F.; Dominy, B.W.; Feeney, P.J. Experimental and computational approaches to estimate solubility and permeability in drug discovery and development setting. *Advanced Drug Delivery Reviews* **2001**, *46*, 3-26, https://doi.org/10.1016/s0169-409x(00)00129-0.
3. Brandán, S.A. Why morphine is a molecule chemically powerful. Their comparison with cocaine. *Indian Journal of Applied Research* **2017**, *7*, 511-528.
4. Rudyk, R.A.; Brandán, S.A. Force field, internal coordinates and vibrational study of alkaloid tropane hydrochloride by using their infrared spectrum and DFT calculations. *Paripex A Indian Journal of Research* **2017**, *6*, 616-623.

5. Romani, D.; Brandán, S.A. Vibrational analyses of alkaloid cocaine as free base, cationic and hydrochloride species based on their internal coordinates and force fields. *Paripex A Indian Journal of Research* **2017**, *6*, 587-602.
6. Iramain, M.A.; Ledesma, A.E.; Brandán, S.A. Analyzing the effects of halogen on properties of a halogenated series of R and S enantiomers analogues alkaloid cocaine-X, X=F, Cl, Br, I. *Paripex A Indian Journal of Research*, **2017**, *6*, 454-463.
7. Brandán, S.A. Understanding the potency of heroin against to morphine and cocaine. *IJSRM, International Journal of Science and Research Methodology* **2018**, *12*, 97-140.
8. Rudyk, R.A.; Checa, M.A.; Guzzetti, K.A.; Iramain, M.A.; Brandán, S.A. Behaviour of N-CH_3 Group in Tropane Alkaloids and correlations in their Properties. *IJSRM, International Journal of Science And Research Methodology* **2018**, *10*, 70-97.
9. Rudyk, R.A.; Checa, M.A.; Catalán, C.A.N.; Brandán, S.A. Structural, FT-IR, FT-Raman and ECD spectroscopic studies of free base, cationic and hydrobromide species of scopolamine alkaloid. *J. Mol. Struct.* **2019**, *1180*, 603-617, https://doi.org/10.1016/j.molstruc.2018.12.040.
10. Iramain, M.A.; Brandán, S.A. Structural and vibrational properties of three species of anti-histaminic diphenhydramine by using DFT calculations and the SQM approach. *Journal: To Chemistry Journal* **2018**, *1*, 105-130.
11. Márquez, M.J.; Iramain, M.A.; Brandán, S.A. *Ab-initio* and Vibrational studies on Free Base, Cationic and Hydrochloride Species Derived from Antihistaminic Cyclizine agent. *International Journal of Science and Research Methodology* **2019**, *11*, 53-87.
12. Manzur, M.E.; Rudyk, R.A.; Brandán, S.A. Evaluating properties of free base, cationic and hydrochloride Species of potent psychotropic 4-Bromo-2,5-dimethoxyphenethylamine drug. *International Journal of Current Advanced Research* **2019**, *8*, 17166-17170.
13. Iramain, M.A.; Ruiz Hidalgo, J.; Brandán, S.A. Predicting properties of species derived from N-(1H-indol-3-ylmethyl)-N,N-dimethylamine, Gramine, a indol alkaloid. *International Journal of Current Advanced Research* **2019**, *8*, 18113-18124.
14. Romani, D.; Ruiz Hidalgo, J.; Iramain, M.A.; Brandán, S.A. Structures, Reactivities and Vibrational Study of Species Derived from the Adrenergic α_2 Receptor Agonist Guanfacine. *International Journal of Science And Research Methodology* **2019**, *12*, 74-98.
15. Manzur, M.E.; Brandán, S.A. S(-) and R(+) Species Derived from Antihistaminic Promethazine Agent: Structural and Vibrational Studies. *Heliyon* **2019**, *5*, https://doi.org/10.1016/j.heliyon.2019.e02322.
16. Márquez, M.J.; Brandán, S.A. DFT study of Species Derived from the Narcotic Antagonist Naloxone, *Biointerface Research in Applied Chemistry* **2020,** *10*, 8096-8116, https://doi.org/10.33263/BRIAC102.096116.
17. Ruiz Hidalgo, J.; Iramain, M.A.; Brandán, S.A. Structural Studies and Spectroscopic properties of Quinolizidine Alkaloids (+) and (-)-Lupinine in different media. *J. Mater. Environ. Sci.* **2019**, *10*, 854-871.
18. Contreras, C.D.; Ledesma, A E.; Zinczuk, J.; Brandán, S.A. Vibrational study of tolazoline hydrochloride by using FTIR-Raman and DFT calculations. *Spectrochim. Acta A* **2011**, *79*, 1710-1714, https://doi.org/10.1016/j.saa.2011.05.041.
19. Romano, E.; Brizuela, A.B.; Guzzetti, K.; Brandán, S.A. An experimental and theoretical study on the hydration in aqueous medium of the anti-hypertensive agent tolazoline hydrochloride. *J. Mol. Struct.* **2013**, *1037*, 393-401, http://dx.doi.org/10.1016/j.molstruc.2013.01.028.
20. Romano, E.; Davies, L.; Brandán, S.A. Structural properties and FTIR-Raman spectra of the anti-hypertensive, clonidine hydrochloride agent and their dimeric species. *J. Mol. Struct.* **2017**, *1133*, 226-235, http://dx.doi.org/10.1016/j.molstruc.2016.12.008.
21. Brandán, S.A. Correlations in hydrochloride drugs with diverse pharmacological activities. Role of N-H···Cl bonds. *Biointerface Research in Applied Chemistry* **2020**, *10*, 5536-5547, https://doi.org/10.33263/BRIAC103.536547.
22. Guzzetti, K.A.; Iramain, M.A.; Rudyk, R.A.; Manzur, M.E.; Brandán, S.A., Vibrational Studies of Species Derived from Potent S(+) and R(-) Ecstasy Stimulant by Using *Ab-initio* Calculations and the SQM Approach. *Biointerface Research in Applied Chemistry* **2020**, *10*, 6783-6809, https://doi.org/10.33263/BRIAC106.67836809.
23. Brandán, S.A. Normal internal coordinates, Force fields and vibrational study of Species Derived from Antiviral amantadine. *Int. J. Quantum Chem*. **2021**, *121*, https://doi.org/10.1002/qua.26425.
24. Smyj, R.; Wang, X-P.; Han, F. Chapter 11-Tramadol Hydrochloride. In: *Profiles of Drug Substances, Excipients, and Related Methodology*. Elsevier Inc.ISSN 1871-5125, Volume 38, **2013;** http://dx.doi.org/10.1016/B978-0-12-407691-4.00011-3.
25. Becke, A.D. Density-functional exchange-energy approximation with correct asymptotic behavior. *Phys. Rev*. **1988**, *A38*, 3098-3100, https://doi.org/10.1103/PhysRevA.38.3098.
26. Lee, C.; Yang, W.; Parr, R.G. Development of the Colle-Salvetti correlation-energy formula into a functional of the electron density. *Phys. Rev*. **1988**, *B37*, 785-789, https://doi.org/10.1103/PhysRevB.37.785.
27. Pulay, P.; Fogarasi, G.; Pongor, G.; Boggs, J.E.; Vargha, A. Combination of theoretical ab initio and experimental information to obtain reliable harmonic force constants. Scaled quantum mechanical (QM)

force fields for glyoxal, acrolein, butadiene, formaldehyde, and ethylene. *Journal of the American Chemical Society* **1983**, *105*, 7037-7047, https://doi.org/10.1021/ja00362a005
28. Rauhut, G.; Pulay, P. Transferable Scaling Factors for Density Functional Derived Vibrational Force Fields. *J. Phys. Chem*. **1995**, *99*, 3093-3100, https://doi.org/10.1021/j100010a019
29. Sundius, T. Scaling of ab-initio force fields by MOLVIB. *Vib. Spectrosc*. **2002**, *29*, 89-95, https://doi.org/10.1016/S0924-2031(01)00189-8.
30. *Tramadol Hydrochloride, European Pharmacopoeia*. seventh ed., European Directorate for the Quality of Medicines & Healthcare (EDQM), Council of Europe, Strasbourg, **2010**; pp. 3118–3119.
31. Kaduk, J.A.; Zhong, K.; Gindhart, A.M.; Blanton, T.N. Crystal structure of tramadol hydrochloride, C16H26NO2Cl. *Powder Diffraction* **2015**, *30*, 242-249, https://doi.org/10.1017/S088571561500041X.
32. Siddaraju, B.P.; Jasinski, J.P.; Golen, J.A.; Yathirajan, H.S.; Raju, C.R. Tramadol hydro-chloride-benzoic acid (1/1). *Acta Crystallogr Sect E Struct Rep Online* **2011**, *67*, o2351-o2351, https://doi.org/10.1107/S1600536811032181.
33. Bag, P.P.; Reddy, C.M. Tramadol Hydrochloride and its Acetonitrile Solvate: Crystal Structure Analysis and Thermal Studies. *Proceedings of the National Academy of Sciences, India Section A: Physical Sciences* **2014**, *84*, 235-242, https://doi.org/10.1007/s40010-013-0118-0.
34. Nielsen, A.B.; Holder, A.J. Gauss View 5.0, User's Reference, GAUSSIAN Inc., Pittsburgh, PA, **2008.**
35. Frisch, M.J.; Trucks, G.W.; Schlegel, H.B.; Scuseria, G.E.; Robb, M.A.; Cheeseman, J.R.; Scalmani, G.; Barone, V.; Mennucci, B.; Petersson, G.A.; Nakatsuji, H.; Caricato, M.; Li, X.; Hratchian, H.P.; Izmaylov, A.F.; Bloino, J.; Zheng, G.; Sonnenberg, J.L.; Hada, M.; Ehara, M.; Toyota, K.; Fukuda, R.; Hasegawa, J.; Ishida, M.; Nakajima, T.; Honda, Y.; Kitao, O.; Nakai, H.; Vreven, T.; Montgomery, J.A.; Peralta, J.E.; Ogliaro, F.; Bearpark, M.; Heyd, J.J.; Brothers, E.; Kudin, K.N.; Staroverov, V.N.; Kobayashi, R.; Normand, J.; Raghavachari, K.; Rendell, A.; Burant, J.C.; Iyengar, S.S.; Tomasi, J.; Cossi, M.; Rega, N.; Millam, J.M.; Klene, M.; Knox, J.E.; Cross, J.B.; Bakken, V.; Adamo, C.; Jaramillo, J.; Gomperts, R.; Stratmann, R.E.; Yazyev, O.; Austin, A.J.; Cammi, R.; Pomelli, C.; Ochterski, J.W.; Martin, R.L.; Morokuma, K.; Zakrzewski, V.G.; Voth, G.A.; Salvador, P.; Dannenberg, J.J.; Dapprich, S.; Daniels, A.D.; Farkas, O.; Foresman, J.B.; Ortiz, J.; Cioslowski, J.; Fox, D.J. Gaussian, Inc., Wallingford CT, **2009**.
36. Miertus, S.; Scrocco, E.; Tomasi, J. Electrostatic interaction of a solute with a continuum. *Chem. Phys.* **1981**, *55*, 117–129, https://doi.org/10.1016/0301-0104(81)85090-2.
37. Tomasi, J.; Persico, J. Molecular Interactions in Solution: An Overview of Methods Based on Continous Distributions of the Solvent. *Chem. Rev*. **1994**, *94*, 2027-2094, https://doi.org/10.1021/cr00031a013.
38. Marenich, A.V.; Cramer, C.J.; Truhlar, D.G. Universal solvation model based on solute electron density and a continuum model of the solvent defined by the bulk dielectric constant and atomic surface tensions. *J. Phys. Chem.* **2009**, *B113*, 6378-6396, https://doi.org/10.1021/jp810292n.
39. Keresztury, G.; Holly, S.; Besenyei, G.; Varga, J.; Wang, A.; Durig, J.R. Vibrational spectra of monothiocarbamates-II. IR and Raman spectra, vibrational assignment, conformational analysis and ab initio calculations of S-methyl-N,N-dimethylthiocarbamate. *Spectrochimica Acta Part A: Molecular Spectroscopy* **1993**, *49*, 2007-2026, https://doi.org/10.1016/S0584-8539(09)91012-1.
40. Michalska, D.; Wysokiński, R. The prediction of Raman spectra of platinum(II) anticancer drugs by density functional theory. *Chemical Physics Letters* **2005**, *403*, 211-217, https://doi.org/10.1016/j.cplett.2004.12.096.
41. Glendening, E.; Badenhoop, J.K.; Reed, A.D.; Carpenter, J.E.; Weinhold, F. NBO 3.1; *Theoretical Chemistry Institute.* University of Wisconsin; Madison, WI, **1996.**
42. Bader, R.F.W. *Atoms in Molecules, A Quantum Theory*. Oxford University Press, Oxford, **1990.**
43. Biegler-Köning, F.; Schönbohm, J.; Bayles, D. AIM2000; A Program to Analyze and Visualize Atoms in Molecules. *J. Comput. Chem.* **2001**, *22*, http://dx.doi.org/10.1002/1096-987X(20010415)22:5%3C545::AID-JCC1027%3E3.0.CO;2-Y.
44. Besler, B.H.; Merz, Jr. K.M.; Kollman, P.A. Atomic charges derived from semiempirical methods. *J. Comp. Chem.* **1990**, *11*, 431-439, https://doi.org/10.1002/jcc.540110404.
45. Ugliengo, P. *MOLDRAW Program*. University of Torino, Dipartimento Chimica IFM, Torino, Italy, **1998**.
46. Parr, R.G.; Pearson, R.G. Absolute hardness: companion parameter to absolute electronegativity. *Journal of the American Chemical Society* **1983**, *105*, 7512-7516, https://doi.org/10.1021/ja00364a005.
47. Ditchfield, R. Self-consistent perturbation theory of diamagnetism. *Molecular Physics* **1974**, *27*, 789-807, https://doi.org/10.1080/00268977400100711.
48. *Experimental available ATR and Raman spectra of topiramate from:* https://spectrabase.com/spectrum/.
49. Minteguiaga, M.; Dellacassa, E.; Iramain, M.A.; Catalán, C.A.N.; Brandán, S.A. Synthesis, spectroscopic characterization and structural study of 2-isopropenyl-3-methylphenol, carquejiphenol, a carquejol derivative with potential medicinal use. *Journal of Molecular Structure* **2018**, *1165*, 332-343, https://doi.org/10.1016/j.molstruc.2018.04.001.
50. Minteguiaga, M.; Dellacassa, E.; Iramain, M.A.; Catalán, C.A.N.; Brandán, S.A. FT-IR, FT-Raman, UV–Vis, NMR and structural studies of carquejyl acetate, a distinctive component of the essential oil from Baccharis trimera (less.) DC. (Asteraceae). *Journal of Molecular Structure* **2019**, *1177*, 499-510, https://doi.org/10.1016/j.molstruc.2018.10.010.